 © 2015 Russian Academy of Sciences and Turpion Ltd

DOI 10.1070/RCR4479

Crystallographic analysis of a series of inorganic compounds †

S V Borisov, S A Magarill, N V Pervukhina

A V Nikolaev Institute of Inorganic Chemistry, Siberian Branch of the Russian Academy of Sciences prosp. Akademika Lavrentieva 3, 630090 Novosibirsk, Russian Federation

The method of crystallographic analysis relies on the mechanical-wave concept that treats the crystalline state as the result of ordering of atomic positions by families of parallel equidistant planes. Using this method, a large set of fluoride, oxide and sulfide structures was analyzed. The pseudo-translational ordering of various atomic groups (including the presence of cation and anion sublattices) in the structures of various classes of inorganic compounds was established. The crucial role of local ordering of heavy cations (coherent assembly) in the structures comprising large cluster fragments (Keggin polyanions, polyoxoniobates, *etc.*) is discussed. The role of symmetry and the regular distribution of heavy atoms in the formation of stable crystal structures, which is to be taken into account in the targeted design, is considered. The universality of configurations of atomic positions in the structures of various classes of inorganic compounds resulting from the ordering mechanism organized by mechanical (elastic) forces is demonstrated.
The bibliography includes 158 references.

Contents

I. Introduction 393
II. Crystallographic analysis method 394
III. Crystallographic analysis of cation matrices in fluoride and oxide structures 394
IV. Crystallographic analysis of sulfides 400
V. Crystallographic analysis of compounds with cluster fragments 412
VI. Principle of coherent assembly of structures with large cluster blocks 415
VII. Conclusion 419

I. Introduction

The method of X-ray diffraction analysis that was developed after the discovery of X-ray diffraction in 1913 provided a tool for the unambiguous determination of the atomic sizes, lengths of different types of chemical bonds, coordination environment, *i.e.*, for calculations of the patterns that have been in part envisioned by chemists at that time. Chemists extrapolated the data obtained for the crystalline state to compounds in solution, which were mostly used in various experiments. Two large areas emerged during the development of the science about the atomic structure of matter.

Studies in one area, which can be referred to as stereochemistry, concern with the detailed analysis of chemical interactions, including coordination numbers, bond lengths, bond angles and, in part, the second coordination sphere. Most modern structural studies are confined to these data, giving some attention to characteristics of the bonds in coordination polyhedra, giving rise in some cases to stringent topological standards (for example, the graph theory [1,2]). Another area of research focuses on the specific features of the crystalline state — a combination of local atomic configurations with a translational lattice, the role of symmetry elements in the structure formation and the geometric similarity of structures of different compositions. In other words, the goal of the latter area of research is to study the mechanisms of crystallization as a widespread phenomenon in the nature. In this field, the international research team has achieved great success [3–8] by treating crystal structures as a combination of plane atomic networks having different configurations. The further development of theses views gave rise to the concept of reticular chemistry [9] and the crystal structure design.[10] Simultaneously, Canadian crystallographer Pearson proposed represening crystal structures as superpositions of plane atomic networks [11] and employed this description as the basis for the classification, which is currently used in the Inorganic Crystal Structure Database (ICSD).[12] Works by Kripyakevich,[13] Smironova [14] and other Russian and foreign researchers [15] also belong to this line of studies. The

S V Borisov Doctor of Physics and Mathematical Sciences, Professor, Chief Researcher at the NIIC SB RAS.
Telephone: +7(383)330–9466, e-mail: borisov@niic.nsc.ru
S A Magarill Candidate of Chemical Sciences, Senior Researcher at the same Institute.
Telephone: +7(383)330–9466, e-mail: svetlana@niic.nsc.ru
N V Pervukhina Candidate of Chemical Sciences, Senior Researcher at the same Institute.
Telephone: +7(383)330–9466, e-mail: pervukh@niic.nsc.ru
Current research interests of authors: crystallography, crystal chemistry of inorganic and complex compounds.

Received 30 June 2014
Uspekhi Khimii **84** (4) 393–421 (2015); translated by T N Safonova

† This review continues a series of reviews dedicated to the International Year of Crystallography [see *Russ. Chem. Rev.* **83** (12) (2014)].

approaches used by these researches developed into separate fields of extensive research.‡

The present review considers the method of crystal structure investigations, which started from geometric studies of atomic arrangements (primarily of the arrangement of heavy metal cations) popular in the 1970s. However, the vast diversity of the sizes and forms of the cells of plane atomic networks found in the structures led to the need to take into account, at least at a qualitative level, the energy criterion controlling the processes in the material world, including universal (for different objects) crystallization processes. In terms of the classical mechanics of wave processes in elastic media, a model of ordering of atomic positions by systems of parallel equidistant planes was formulated. The fixation of atoms in the planes results in the loss of individual degrees of freedom, which accounts for the paradox of crystallization: the ordering of material particles does not require energy and, on the contrary, leads to the energy release. In order to validate this hypothesis, algorithms referred to as the crystallographic analysis technique were devised, and hundreds of crystal structures of inorganic compounds, for which the energy effect of crystallization is most significant, were investigated. The main advances include:

— several types of stable atomic sublattices for structures of different compositions were found;

— it was shown that the ordering of different atomic groups in the structure occurs independently to form the translational unit cell common for these groups;

— the effect of ordering of atomic groups with atoms linked by strong chemical bonds to represent them as a whole objects was established;

— the phenomenon of coherent assembly was revealed, when the spatial ordering of atoms in fragments of the structure is responsible for their arrangement.

The proposed method has no analogues in the area of investigations of the structure of matter, although it intersects, to a certain extent, with crystal chemical, topological and modular approaches.

II. Crystallographic analysis method

Studies of the factors responsible for the crystal formation for a wide range of heavy metal fluorides and oxides and other inorganic compounds[16] have brought about the mechanical-wave concept of the crystalline state, according to which the long-range order arises from the ordering of atomic positions by systems of parallel equidistant planes [former crystallographic planes (*hkl*) of the structure]. The crystallographic analysis technique, which was developed on the basis of this concept and basics of crystallography,[16] involves the establishment of all significant signs of ordering of atomic positions in the structures. For this purpose, crystallographic planes are tested for the density of atoms, which directly correlates with the intensity of X-ray reflections from these planes and has the maximum value if the centres of all atoms lie exactly in the planes.

Three systems of noncoplanar crystallographic planes characterized by the highest density of atoms intersect to form a three-dimensional lattice of points of intersection (lattice points), the number of which per unit cell of the structure is equal to the determinant from the h, k, l indices of these planes.[16] Since all three systems have high atom density, the atomic positions will be located in the vicinity of the points of their intersection, *i.e.*, they form a pseudotranslational sublattice. The existence of pseudotranslations means that different atoms can be located at the lattice points and their positions not necessarily exactly coincide with the lattice points. Since the range of interplanar spacing for the planes characterized by the maximum density of atoms is rather narrow and comparable with the minimum interatomic contacts, the analysis is usually confined to the range $2 \leqslant d_{hkl} \leqslant 4.5$ Å. It should be noted that the strongest interatomic bonds are often located in these planes. Therefore, it can be stated that the structure has a stable skeleton represented by this pseudotranslational lattice.

Since any three noncoplanar planes give a sublattice, whereas the planes with high density (*i.e.*, with a high degree of ordering of atomic positions) can be more than three, the problem of the adjustment of different pseudotranslational sublattices of atoms within the structure is solved by the formation of the common translational lattice. The role of the symmetry elements is to make identical the crystallographic planes in different orientations. As a consequence, in the structures with, for example, orthorhombic symmetry the densely filled (hkl) plane together with the symmetry-related ($\bar{h}kl$) and ($h\bar{k}l$) planes determine the skeletal sublattice of the structure.

It follows from the mechanical-wave concept of the crystalline state that the ordering of atoms of heavy elements has a priority over the ordering of atoms of light elements and in structures of many compounds, in particular in oxides and fluorides, the ordering of heavy and moderate-mass cations determines the 'appearance' of the crystal structure. The practice of crystallographic analysis also showed that different atomic groups can be ordered by means of different sets of crystallographic planes. This fact can be reasonably attributed to the spontaneous character of the onset of crystallization. Atoms can be arranged in groups based both on the chemical characteristics (for example, cations and anions are arranged in separate groups) and the size: large cations (Tl^+, Cs^+, Rb^+, *etc.*) are often ordered together with both other cations involved in the structure and commensurate anions (O^{2-}, S^{2-}, Cl^-, *etc.*). If the ordering of different atomic groups or the ordering by different systems of planes does not lead to a single translational lattice of reasonable sizes (*i.e.*, pseudotranslational sublattices prove to be incommensurate), quasicrystalline structures (modulated,[17] vernier, *etc.*[18]) are formed.

III. Crystallographic analysis of cation matrices in fluoride and oxide structures

The choice of inorganic oxides and fluoride for the validation of the crystallographic analysis technique is dictated mainly by two factors:

— numerous structures of any symmetry and complexity having various sets of cations are known for these classes of compounds;

— the problem can be limited to studies of three-dimensional configurations of only cation positions (geometry of cation matrices) assuming that lighter anions play a minor role in the structure formation.

‡ Certain results obtained in this area are considered in anniversary special issues of the journals *Struct. Chem.* **23** 977 (2012) dedicated to S Andersen on the occasion of his anniversary and *Can. Mineral.* **50** 387 (2012), which is a tribute to E Makovicky.

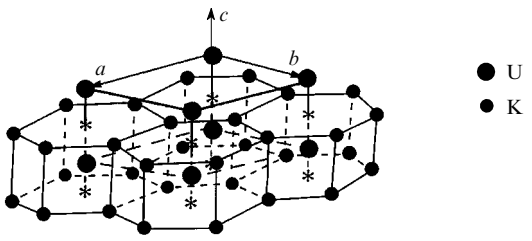


Figure 1. Cation matrix of the β-K_2UF_6 structure type. Vacancies in the potassium cation network are marked with an asterisk.[19]

About a hundred structure types of both oxide and fluoride compounds were analyzed, many of which proved to be structurally similar. In the first approximation, the three-dimensional configurations of cation positions in these structures can be divided into three groups:

— structures, the geometry of which is similar to face-centred cubic (F_c) unit cells;

— structures similar to body-centred cubic (I_c) unit cells;

— structures having hexagonal single-layer and double-layer sublattices often containing vacant lattice points; an example is the cation matrix of the β-K_2UF_6 structure (space group $P\bar{6}2m$, $Z = 1$, $a = 6.553$, $c = 3.749$ Å), in which potassium cations form planar networks composed of hexagons perpendicular to the $\bar{6}$ symmetry axis that alternate with trigonal networks of uranium cations, the latter occupying the sites above the centres of the hexagons belonging to the network of potassium cations (Fig. 1).

III.1. Cation matrices in fluoride structures

Let us consider the crystallographic analysis technique for three fluorides with typical cation sublattices. Table 1 gives, along with the data on these structures, the transformation matrices from the unit cell parameters to the parameters of the cation subcell, as well as the values of the determinant of this matrix indicating the fraction of the volume of the F_c subcell in the volume of the translational unit cell. Crystallographic planes with a high density of cations [characterized by the relative density (ρ_{hkl}) normalized to unity from the calculations using the KAP–PLATS programme package [15] or by a high scattering amplitude of cations (F_c)] and the indices of the skeletal planes (hkl) with respect to the cation sublattice $(hkl)_c$ for the fluoride structures under consideration are given in Table 2.

$Na_5Zr_2F_{13}$. The relationship between the subcell parameters a_c, b_c, c_c and the unit cell parameters of the structure can be easily obtained using the transformation matrix:

$$\boldsymbol{a}_c = \frac{3}{7}\boldsymbol{a} + \frac{2}{7}\boldsymbol{c};$$

$$\boldsymbol{b}_c = \boldsymbol{b};\ \boldsymbol{c}_c = -\frac{1}{7}\boldsymbol{a} + \frac{4}{7}\boldsymbol{c}$$

(these relationships were obtained using software described by Gromilov *et al.*[21]). The numerical values of the subcell parameters are given in Table 1. Figure 2 presents the projection of the cation positions in the $Na_5Zr_2F_{13}$ structure onto the xz plane and its cross-sections by the skeletal planes (401) and $(20\bar{3})$, which form, together with the (020) planes, the cation sublattice points. The number of these lattice points per unit cell is 28 [the determinant of the

Table 1. Crystallographic data for $Na_5Zr_2F_{13}$, Na_3MnF_6 and K_5ThF_9.

$Na_5Zr_2F_{13}$ (Refs 20, 21) (space group $C2/m$)	Na_3MnF_6 (Ref. 22) (space group $P2_1/n$)	K_5ThF_9 (Ref. 23) (space group $Cmc2_1$)
Unit cell parameters:	Unit cell parameters:	Unit cell parameters:
$a = 11.62$, $b = 5.49$, $c = 9.44$, $\beta = 97.7$,	$a = 5.471$, $b = 5.683$, $c = 8.073$, $\beta = 89.0$	$a = 7.848$, $b = 12.84$, $c = 10.78$,
$Z = 2$, $N_c = 14$, $V_c/V_0 = 2/7$	$Z = 2$, $N_c = 8$, $V_c/V_0 = 1/4$	$Z = 4$, $N_c = 24$, $V_c/V_0 = 1/48$
Transformation matrix to the subcell:	Transformation matrix to the subcell:	Transformation matrix to the subcell:
3/7 0 2/7	1/2 1/2 0	0 1/4 1/6
0 1 0	−1/2 1/2 0	0 −1/4 1/6
−1/7 0 4/7	0 0 1/2	1/4 0 0
Parameters of the cation subcell:	Parameters of the cation subcell:	Parameters of the cation subcell:
$a_c = 5.23$, $b_c = 5.49$, $c_c = 5.30$,	$a_c = 3.95$, $b_c = 3.95$, $c_c = 4.04$,	$a_c = 3.68$, $b_c = 3.68$, $c_c = 1.96$,
$\beta_c = 88.6$	$\alpha_c = 90.5$, $\beta_c = 89.5$, $\gamma_c = 88.0$	$\gamma_c = 121.53$

Note. Here and in other tables, the unit cell parameters a, b, c, d_{hkl} are given in Ångströms, the angles α, β, γ are expressed in degrees; the following notations are used: Z is the number of formula units per unit cell, N_c is the number of cations per unit cell, V_c/V_0 is the fraction of the subcell volume in the unit cell volume.

Table 2. Results of crystallographic analysis of the $Na_5Zr_2F_{13}$, Na_3MnF_6 and K_5ThF_9 structures.

$Na_5Zr_2F_{13}$ (Refs 20, 21)				Na_3MnF_6 (Ref. 22)								K_5ThF_9 (Ref. 23)			
hkl	d_{hkl}	ρ_{hkl}	$(hkl)_c$	hkl	d_{hkl}	$F_c > 60$	$(hkl)_c$	hkl	d_{hkl}	$F_c > 60$	$(hkl)_c$	hkl	d_{hkl}	$F_c > 400$	$(hkl)_c$
112	3.11	0.98	111	020	2.84	83	110	220	1.97	73	200	040	3.21	436	$1\bar{1}0$
$\bar{3}11$	3.06	0.97	$\bar{1}11$	112	2.84	89	101	024	1.64	66	112	221	3.20	438	–
020	2.74	1.00	020	$\bar{1}12$	2.80	88	011	204	1.64	72	$1\bar{1}2$	202	3.17	506	–
401	2.62	0.95	200	200	2.74	90	$1\bar{1}0$	$\bar{2}04$	1.61	71	$\bar{1}12$	023	3.14	546	100
203	2.65	0.95	002	004	2.02	81	002	312	1.60	69	$2\bar{1}1$	400	1.96	523	001
								$\bar{3}12$	1.59	69	$\bar{2}11$	006	1.80	437	110
												423	1.66	430	101

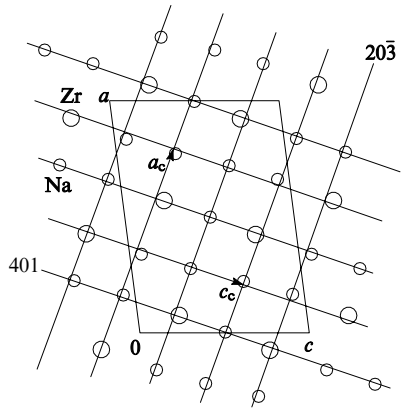


Figure 2. Cation positions in the $Na_5Zr_2F_{13}$ structure projected onto the *xz* plane and its cross-sections by the perpendicular (401) and ($20\bar{3}$) planes.§

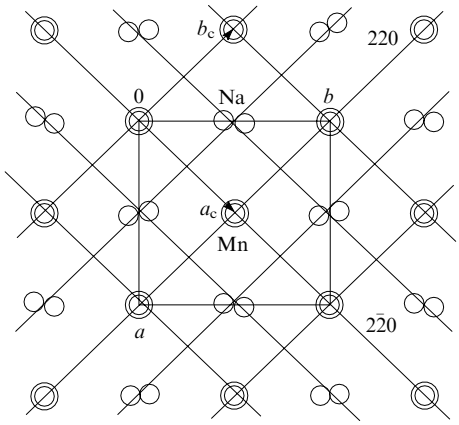


Figure 3. Cation positions in the Na_3MnF_6 structure projected onto the *xy* plane and its cross-sections by the (220) and ($2\bar{2}0$) planes.[22]

indices of the (401), ($20\bar{3}$) and (020) planes], the cations occupy one-half of the lattice points, which is characteristic of *F*-cubic unit cells divided by the (200), (020) and (002) planes into eight subcells, in which four of the eight vertices are occupied. It should be noted that sodium and zirconium cations, which differ in chemical and crystal-chemical characteristics, as well as in the mass and, in part, in the size, form a rather regular face-centred pseudocubic sublattice. Thus, the monoclinic structure of $Na_5Zr_2F_{13}$ has a cation skeleton as a regular pseudocubic sublattice.

Na_3MnF_6. The crystallographic analysis of the structure of this fluoride (see Table 1, 2) showed that the (220) planes, the symmetry-related ($2\bar{2}0$) planes and the (004) planes form a sublattice of points haveing a nearly cubic subcell with the parameter ~2 Å. Sodium and manganese cations occupy a part of these lattice points according to the law of the *I*-unit cell, the parameters of which are rather close to those of the cubic unit cell. The vector relations between the parameters can be seen in Fig. 3, which presents the projection of the cation positions onto the *xy* plane and the vectors $\boldsymbol{a}_c$ and $\boldsymbol{b}_c$. The third parameter ($\boldsymbol{c}_c = 1/2\,c$) is virtually perpendicular to the plane of the projection ($\beta = 89°$). All cation planes of the sublattices, in addition to the coordinate planes (220) and (004), have a high density of cations (intense reflections, see Table 2), which is indicative of the cation skeleton of the structure with the *I*-lattice geometry.

K_5ThF_9. The crystallographic analysis of the structure of this fluoride showed that the cation sublattice is pseudohexagonal and has one-half vacant lattice points (see Tables 1 and 2). Figure 4 presents the projection of cation positions onto the *yz* plane and the network of cation sublattice points. It is evident that the alternation of lattice points occupied by cations with vacant points along the c_c axis in the cation sublattice is a necessary condition because the contacts between cations with a distance of 1.96 Å are impossible in this structure. Taking into account this limitation, all 24 cation sublattice points accessible for filling in the unit cell are occupied by potassium and thorium cations, which form planar networks perpendicular to the *x* axis separated by the distance of $1/4\,a$. Structures characterized by short translations of sublattices and, consequently, the regular alternation of vacant and occupied lattice points along these translations occur rather often.[16]

§ Figures 2–7, 8*c*, 15, 16, 23, 26 and 28 were prepared by the authors specially for this review.

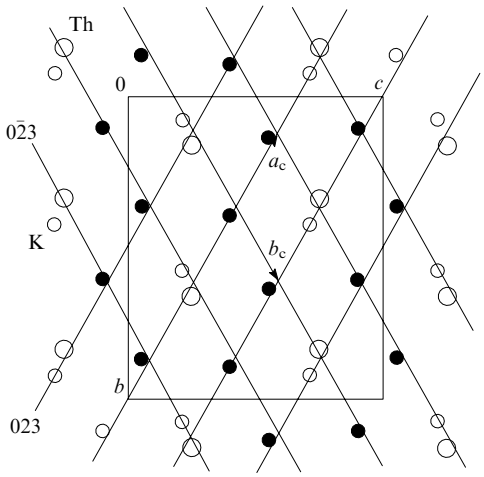


Figure 4. Cation positions in the K_5ThF_9 structure projected onto the *yz* plane and its cross-sections by the (023) and ($0\bar{2}3$) planes. Empty and filled circles indicate the positions at two different heights.

Cation matrices of other fluorides. It is known that at small values of d_{hkl} (smaller than the minimum interatomic contacts) the maximum density of atoms in the (*hkl*) planes decreases proportionally to d_{hkl}.[16] However, these planes can be competitive in the structure formation due to the more strict ordering of atomic positions. For example, this refers to the (*hkl*) planes that coincide with the mirror planes. Atoms can either lie exactly in this plane or be located from this plane at a distance not smaller than their radii. Evidently, if the structure contains a short (~4 Å) translation and the mirror plane perpendicular to this translation, the centres of all atoms should be located in these planes separated by one-half of the short translation (~2 Å). A rather large number of such structures are known.[16]

Data on the cation sublattices for the fluorides under study are given in Table 3. The analysis of these data showed that the values of the unit cell parameters for each type of cation sublattice vary in a rather narrow range and

Table 3. Cation sublattice parameters in structures of heavy metal fluorides.[16, 24]

Compound	Space group	V_c/V_0	Cation sublattice parameters					
			a_c/Å	b_c/Å	c_c/Å	α_c/deg	β_c/deg	γ_c/deg
F-Centred unit cell of cations								
CaF_2	$Fm3m$	1	5.46	5.46	5.46	90.0	90.0	90.0
KTb_3F_{10}	$Fm3m$	1/8	5.81	5.81	5.81	90.0	90.0	90.0
Ca_2LuF_7	$I4/m$	2/15	5.48	5.48	5.45	90.0	90.0	90.0
$K_{17}Gd_{47}F_{158}$	$Immm$	1/16	5.76	5.76	5.83	90.0	90.0	90.1
Li_6BeZrF_{12}	$I4_1/amd$	1/8	4.65	4.65	4.65	90.0	90.0	90.0
$LiYbF_4$	$I4_1/a$	1/2	5.13	5.13	5.29	90.0	90.0	90.0
Li_2CaUF_6	$I4m2$	1/2	5.23	5.23	5.51	90.0	90.0	90.0
KYF_4	$P3_1$	1/9	5.77	5.77	5.77	89.4	89.4	89.4
$K_7Th_6F_{31}$	$R\bar{3}$	4/39	6.01	6.01	6.00	90.2	89.8	90.3
$Ca_{14}Y_5F_{43}$	$R\bar{3}$	4/57	5.47	5.47	5.46	88.9	89.0	88.8
Pb_3ZrF_{10}	$Cmcm$	1/4	5.36	6.41	5.91	90.0	90.0	90.0
KHo_3F_7	Cm	1/6	5.38	5.62	5.62	89.2	91.3	88.7
Li_2TbF_6	$P2_1/c$	1/3	5.06	5.33	4.96	90.0	90.0	93.8
TlOF	$I\bar{4}3m$	1/8	5.40	5.40	5.40	90.0	90.0	90.0
YOF	$R\bar{3}m$	2/3	5.40	5.40	5.40	89.4	89.4	89.4
$Pb_8Y_6F_{32}O$	$R\bar{3}$	2/27	5.75	5.69	7.77	89.9	89.3	90.1
$YbTl_2O_5F$	$Pbcn$	1/3	4.79	5.48	5.15	90.0	90.0	90.0
ScOF	$P2_1/c$	1	5.17	5.15	5.25	90.0	99.4	90.0
I-Centred unit cell of cations								
Cs_3TbF_7	$Fm3m$	1/8	4.90	4.90	4.90	90.0	90.0	90.0
Cs_3KYF_6	$Fm3m$	1/8	4.72	4.72	4.72	90.0	90.0	90.0
Rb_2NaErF_6	$Fm3m$	1/8	4.43	4.43	4.43	90.0	90.0	90.0
K_3InF_6	$Fm3m$	1/64	4.43	4.43	4.43	90.0	90.0	90.0
Rb_3TlF_6	$I4/mmm$	1/4	4.87	4.87	4.89	90.0	90.0	90.0
Rb_3ErF_6	$I4_1/amd$	1/32	4.68	4.68	4.68	90.0	90.0	90.0
K_3NaThF_6	$P3$	1/3	4.49	4.49	4.49	89.2	89.2	89.2
Na_2UF_6	$P3$	1/3	4.27	4.27	4.27	91.0	91.0	91.0
$RbPaF_6$	$Cmma$	1/4	6.01	4.02	5.86	90.0	90.0	90.0
$K_5Hf_3F_{17}$	$Pnam$	1/18	4.18	4.43	5.06	90.0	90.0	90.0
$KHoBeF_6$	$P2_1/m$	1/3	4.31	4.31	4.33	87.2	87.2	85.0
Hexagonal unit cell of cations								
β-K_2UF_6	$P\bar{6}2m$	1	6.55	6.55	3.75	90.0	90.0	120.0
Rh_2UF_6	$Cmcm$	1/4	6.96	6.95	3.80	90.0	90.0	120.0
$(NH_4)_2CeF_6$	$Pbcn$	1/4	7.03	7.00	3.72	90.0	90.0	120.1
K_2ZrF_6	$C2/c$	1/4	6.57	6.60	3.47	89.8	90.3	119.9
KSc_2F_7	$Cmmm$	1/2	6.24	6.54	4.03	90.0	90.0	121.6
β-$K_2Yb_2F_7$	$P2$	1	6.53	6.43	4.22	90.0	90.0	115.9
K_2GdF_5	$Pnam$	1/4	6.34	6.62	3.69	90.0	90.0	121.5
K_2SmF_5	$Pna2_1$	1/4	6.33	6.62	3.75	90.0	90.0	120.5
$BaTm_2F_8$	$C2/m$	1/2	6.93	6.27	4.24	84.8	90.0	123.5
$BaLu_2F_8$	$Pnma$	1/8	6.46	6.89	4.04	90.0	90.0	122.2
$Rh_5Zr_4F_{21}$	$P2_1$	1/6	6.60	6.60	4.33	87.5	87.5	116.6

they are evidently determined by a particular cation composition. The unit cell volume of the cation sublattice can coincide with the unit cell volume of the structure (for example, in CaF_2) or be a certain rational fraction of this volume (for example, in cubic K_3InF_6 this fraction is 1/64, *i.e.*, the linear parameter of the cation sublattice is four times smaller than the unit cell parameter of the structure). The structures with the cation *F*-sublattice comprise almost one-half of all characterized structure, which reflects the tendency of cations to form close-packed and highly symmetric structures. It should be noted that the cation subcell of β-K_2UF_6 double-centred at the base was taken as the reference for the cation hexagonal subcells. Therefore, the parameters a and b of the primitive hexagonal subcell shown in Fig. 4 are $\sqrt{3}$ times smaller.

III.2. Cation matrices in oxide structures

In traditional crystal chemistry, the structures of fluorides and oxides are considered as related due to the almost equal sizes of F^- and O^{2-} cations. The crystallographic analysis based on the results of investigations of a rather representative set of structures with different cation compositions[24–27] confirms this fact. Thus, the distribution over three types of cation sublattices — F_c, I_c and hexagonal — is approximately the same as that in the fluoride structures. Let us consider three typical examples.

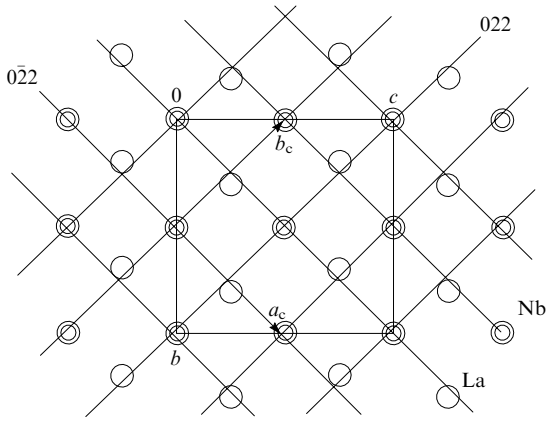


Figure 5. Cation positions in the La_3NbO_7 structure projected onto the *yz* plane and its cross-sections by the (022) and (0$\bar{2}$2) planes.

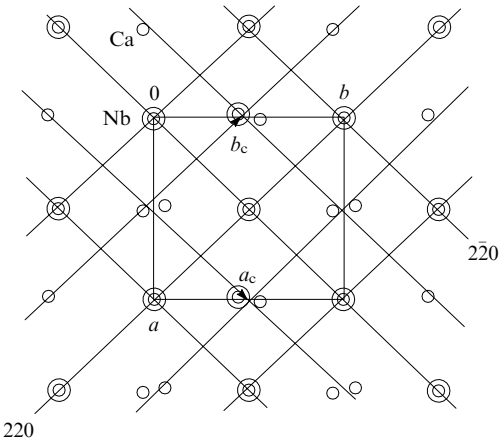


Figure 6. Cation positions in the Ca_2NdNbO_6 structure projected onto the *xy* plane and its cross-sections by the (220) and (2$\bar{2}$0) planes.

La_3NbO_7. In the orthorhombic La_3NbO_7 structure, the cation matrix has a F_c-subcell, as can be easily seen in the *yz* projection of the cation positions (Fig. 5, Tables 4 and 5). The skeletal planes (022), (0$\bar{2}$2) and (400) divide the structure into nearly cubic blocks with the edge of $\sim$2.75 Å. In the pseudocubic subcell formed by eight such blocks, lanthanum and niobium cations occupy one-half of sublattice points arranged according to the *F*-lattice. All other 'intense' cation planes also belong to this unit cell (see Table 5).

Ca_2NdNbO_6. An analysis of the monoclinic structure of this oxide showed that it contains a pseudocubic I_c-subcell of cations (Fig. 6, Tables 4 and 5). As in the previous example, the skeletal planes (220), (2$\bar{2}$0) and (004) divide the structure into cubic blocks with the edge of $\sim$2.0 Å. In the pseudocubic subcell consisting of eight blocks, the cations occupy 1/4 of the vertices according to the *I*-lattice. All eight cations in the unit cell of the Ca_2NdNbO_6 structure are distributed over four *I*-sublattices. It should be noted that the oxide Ca_2NdNbO_6 is isostructural with Na_3MnF_6 (see above). Despite the totally different atomic compositions, the cation matrices in the structures have the same geometry.

$K_3Nb_6P_4O_{26}$. The orthorhombic structure of this oxide contains a hexagonal subcell of cations, eight pseudohexagonal networks of cations being located perpendicular to

Table 4. Crystallographic data for La_3NbO_7, Ca_2NdNbO_6 and $K_3Nb_6P_4O_{26}$.

La_3NbO_7 (Ref. 26) (space group *Cmcm*)	Ca_2NdNbO_6 (Ref. 26) (space group $P2_1/n$)	$K_3Nb_6P_4O_{26}$ (Ref. 27) (space group *Pnma*)
Unit cell parameters: $a = 11.167$, $b = 7.629$, $c = 7.753$, $Z = 4$, $N_c = 16$, $V_c/V_0 = 1/4$	Unit cell parameters: $a = 5.62$, $b = 5.88$, $c = 8.11$, $\beta = 90.2$ $Z = 2$, $N_c = 8$, $V_c/V_0 = 1/4$	Unit cell parameters: $a = 14.75$, $b = 31.60$, $c = 9.39$, $Z = 8$, $N_c = 104$, $V_c/V_0 = 1/104$
Transformation matrix to the subcell: 0 1/2 1/2 0 −1/2 1/2 1/2 0 0	Transformation matrix to the subcell: 1/2 1/2 0 −1/2 1/2 0 0 0 1/2	Transformation matrix to the subcell: 1/13 0 5/13 2/13 0 −3/13 0 1/8 0
Parameters of the cation subcell: $a_c = 5.439$, $b_c = 5.439$, $c_c = 5.583$, $\gamma_c = 89.1$	Parameters of the cation subcell: $a_c = 4.07$, $b_c = 4.07$, $c_c = 4.06$, $\beta_c = 87.4$	Parameters of the cation subcell: $a_c = 3.79$, $b_c = 3.14$, $c_c = 3.95$, $\gamma_c = 116.24$

Table 5. Results of crystallographic analysis of the La_3NbO_7, Ca_2NdNbO_6 and $K_3Nb_6P_4O_{26}$ structures.

La_3NbO_7 (Ref. 26)				Ca_2NdNbO_6 (Ref. 26)				$K_3Nb_6P_4O_{26}$ (Ref. 27)			
hkl	d_{hkl}	$F_c > 500$	$(hkl)_c$	*hkl*	d_{hkl}	$F_c > 150$	$(hkl)_c$	*hkl*	d_{hkl}	$F_c > 1000$	$(hkl)_c$
202	3.18	691	111	020	2.94	194	1$\bar{1}$2	080	3.95	1446	001
220	3.15	613	1$\bar{1}$1	$\bar{1}$12	2.87	216	011	302	3.39	1140	100
400	2.79	620	002	112	2.87	217	101	50$\bar{1}$	2.81	1485	010
022	2.72	608	200	200	2.81	222	1$\bar{1}$0	382	2.57	1042	101
004	1.94	618	220	220	2.03	172	200	58$\bar{1}$	2.29	1249	011
224	1.65	503	311	004	2.03	202	002	0160	1.97	1510	002
620	1.67	417	1$\bar{1}$3	$\bar{2}$04	1.65	181	$\bar{1}$12				
404	1.59	514	222	204	1.64	185	1$\bar{1}$2				
				$\bar{3}$12	1.63	173	$\bar{2}$11				
				312	1.63	175	2$\bar{1}$1				

the long translation ($b = 31.60$ Å). The skeletal cation planes (302), (50$\bar{1}$) and (080) (see Tables 4 and 5) divide the unit cell of the structure into 104 subcells (det{302/50$\bar{1}$/080}) and this is the number of cations per unit cell. Figure 7 presents the projection of the cation positions onto the *xz* plane and shows its cross-sections by the perpendicular (302) and (50$\bar{1}$) planes, which form a network of pseudohexagonal cation sublattice points in its basis $x_c y_c$ plane. In this sublattice, heavy niobium and phosphorus cations are most regularly arranged; the latter ions are in fact the centres of mass of rigid groups of atoms [PO_4], resulting in their higher status in the structure formation. Considerable deviations of the relatively light potassium cations from the sublattice points are not critical for the structure.

Cation sublattices of other oxides. As mentioned above, the structures of oxides and fluorides have similar types of cation sublattices and the latter have similar parameters. The data on the cation sublattices in the structures of complex oxides investigated by our research group are given in Table 6.

To sum up, let us note that the crystallographic analysis revealed the pseudotranslational ordering of cation positions in all structures. This is manifested in the formation of cation sublattices having parameters of the order of the closest intercationic contacts. Cations with different sizes, charges and masses are involved in this ordering; however, heavy cations are, as a rule, responsible for this process.

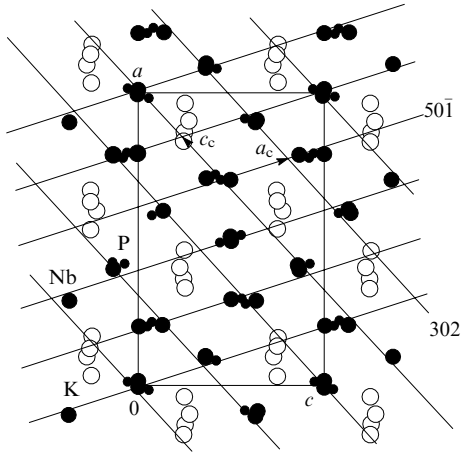


Figure 7. Cation positions in the $K_3Nb_6P_4O_{26}$ structure projected onto the *xz* plane and its cross-sections by the (302) and (50$\bar{1}$) planes.

Table 6. Cation sublattice parameters in niobate and tantalate structures.[16, 24]

Compound	Space group	V_c/V_0	Cation sublattice parameters					
			a_c/Å	b_c/Å	c_c/Å	α_c/deg	β_c/deg	γ_c/deg
F-Centred unit cell of cations								
$GdTaO_4$	$P2/a$	1	5.36	5.51	5.17	90.0	96.7	90.0
$NdTaO_4$	Pa	1	5.41	5.60	5.24	90.0	96.8	90.0
β-$LaTaO_4$	$P2_1/c$	1/2	4.90	6.00	5.58	90.0	90.0	91.5
α-$LaTaO_4$	$A2_1am$	1/2	4.72	6.15	5.66	90.0	90.0	92.2
$LaNbO_4$	$I2/a$	1/2	5.59	5.21	5.76	90.0	90.0	94.1
$YNbO_4$	$C2/c$	1/2	5.07	5.30	5.47	90.0	90.0	85.4
Y_3TaO_7	$C222_1$	1/4	5.26	5.26	5.24	90.0	90.0	89.8
Sm_2ScTaO_7	$Fd3m$	1/8	5.24	5.24	5.24	90.0	90.0	90.0
Na_3TaF_8	$C2/c$	1/4	5.61	4.95	5.38	90.0	90.0	88.2
Li_3TaO_4	$P2/n$	1/6	4.25	4.25	4.17	90.0	90.0	90.2
$Ag_2Nb_2O_5F_2$	$Ima2$	1/4	5.34	5.34	5.23	90.0	90.0	92.0
$Na_2Ta_2O_5F_2$	$C2/m$	1/8	5.14	5.24	5.23	90.0	90.0	89.0
$(Sr,Li)_2TaO_2O_6F$	$Fd3m$	1/8	5.23	5.23	5.23	90.0	90.0	90.0
$Pb_{1.49}Ta_2O_{6.28}$	$Fd3m$	1/8	5.28	5.28	5.28	90.0	90.0	90.0
$ZnNb_2O_6$	$Pbcn$	1/3	4.73	5.73	5.04	90.0	90.0	90.0
$Mg_2Nb_6O_{11}$	$P3m1$	1/3	4.28	4.28	4.28	89.6	89.7	89.7
K_2NbF_7	$P2_1/c$	1/3	6.00	6.00	5.90	90.0	90.0	90.4
$K_2NbO_2 \cdot H_2O$	$C2$	1/3	6.31	6.31	6.07	87.2	92.9	90.0
I-Centred unit cell of cations								
Pb_2ScTaO_6	$Fm3m$	1/8	4.07	4.07	4.07	90.0	90.0	90.0
Sr_2TmNbO_6	$P2nn$	1/4	4.10	4.10	4.10	90.0	90.0	89.8
$K_2NaNbO_2F_4$	$Fm3m$	1/8	4.23	4.23	4.23	90.0	90.0	90.0
Na_3NbOF_6	$P2_12_12_1$	1/8	4.04	4.04	4.23	90.0	90.0	91.2
$(NH_4)_3Ta(O_2)_2F_4$	$Fm3m$	1/8	4.72	4.72	4.72	90.0	90.0	90.0
$MgTa_2O_6$	$P4_2/mnm$	1/3	4.42	4.72	3.07	90.0	90.0	90.0
$CaTa_2O_6$	$Pm\bar{3}$	1/6	3.89	3.89	3.89	90.0	90.0	90.0
$SeNb_2F_{14}$	$P2_1/c$	1/6	6.47	5.80	5.12	90.0	90.0	98.1
$Mg_4Ta_2O_9$	$P\bar{3}c1$	1/6	3.79	3.79	3.79	85.9	94.1	94.1
$Ba_3SrTa_2O_9$	$P6_3/mmc$	1/6	4.34	4.34	4.34	88.9	91.1	91.1
K_2NbOF_5	$P4/nmm$	1/4	4.33	4.33	4.49	90.0	90.0	90.0
K_2NbO_3F	$I4/mmm$	1/3	3.96	3.96	4.42	90.0	90.0	90.0

Table 6 (continued).

Compound	Space group	V_c/V_0	Cation sublattice parameters					
			a_c/Å	b_c/Å	c_c/Å	α_c/deg	β_c/deg	γ_c/deg
Hexagonal unit cell of cations								
$SrNb_2O_6$	$P2_1/c$	1/4	5.59	6.16	3.86	90.0	90.0	117.0
$BaNb_2O_6$	$P2_1/c$	1/2	6.05	6.03	3.95	90.3	90.0	120.1
$BiNbTiO_6$	$P\bar{1}$	1/16	4.93	7.12	3.79	90.0	90.0	110.0
$La_2TaO_4Cl_3$	$Pmmn$	1/12	5.22	5.18	3.94	90.0	90.0	119.7
$NaTaGeO_5$	$C2/c$	1/4	5.63	5.60	3.71	104.8	104.8	105.0
Li_2NbF_6	$P\bar{3}/m$	1	4.96	4.96	4.61	90.0	90.0	120.0

The fact of the pseudotranslational ordering confirms the mechanical-wave concept of the crystalline state [16, 28] because it is a direct consequence of the ordering of atoms by systems of parallel planes.

IV. Crystallographic analysis of sulfides

Crystal structures of sulfides and sulfosalts are characterized by diverse cation compositions.[29] Crystal chemical studies of these compounds were in part performed and systematically considered by disciples and followers of the school of N V Belov [30] at the end of the 20th century. Currently, the international research team headed by Makovicky are taking an active part in the continuation of these studies.[31–33] Many of these investigations were devoted to natural samples — minerals. In some cases, their artificial analogues were synthesized for the sake of convenience. Mineralogists systematized suflosalts based on the chemical composition and the 'modular analysis', which treats the structures as combinations of blocks of simple typical structures [sphalerite (ZnS), galena (PbS), *etc.*].[31]

First studies of compounds containing sulfur anions by the crystallographic analysis method were performed for simple compounds containing one type of cations. It is known that such compounds tend to crystallize in the sphalerite (ZnS) or galena (PbS) structure types, which are characterized by the same distribution of both cation and anion positions to form face-centred cubic lattices with the parameter ~5. Å. In the sphalerite structure type, the cation and anion *F*-lattices are shifted with respect to each other by 1/4 of the body diagonal of the cubic unit cell, so that the cations are located in the centres of anionic tetrahedra (and *vice versa*, anions are in the centres of the cationic tetrahedra). In the PbS structure type, the lattices as shifted by one-half of the body diagonal, and the cations are located in the centres of anionic octahedra (anions are in the centres of cationic octahedra). The larger mass and bulkiness compared to those of the fluorine and oxygen atoms are the factors that increase the role of sulfur anions in the structure formation. As a result, the structures of sulfides are composed of 'independent' orderings of cations and anions. This was demonstrated by the crystallographic analysis of first simple structures.[34]

Thus, in the orthorhombic structure of one of the modifications of Tm_2S_3 (*Pnma*, $Z = 4$, $a = 10.479$, $b = 3.805$, $c = 10.353$ Å),[34] the (103), (301) and (020) planes with 16 sublattice points in the unit cell proved to be the skeletal planes of the cation sublattice, whereas the (302), ($\bar{3}02$) and (020) planes with 24 sublattice points in the unit cell are the skeletal planes for the anions (the latter can be found by calculating the intensities of X-ray reflections only for sulfur atoms). Figure 8 *a*,*b* shows the projections of the cation and anion positions and the networks of the cation and anion sublattices in the Tm_2S_3 structure. All lattice points accessible for filling are occupied, and this number is exactly one-half of a total of lattice points in both subcells, because the occupied and vacant sites alternate along the *b* translation $b_c = 1/2\,b = 1.90$ Å.

The impression that the orderings of cations are independent of anion orderings is evidently absurd since a particular environment, for example of cations by anions, should occur in the structure. As can be seen in Fig. 8 *c*, the

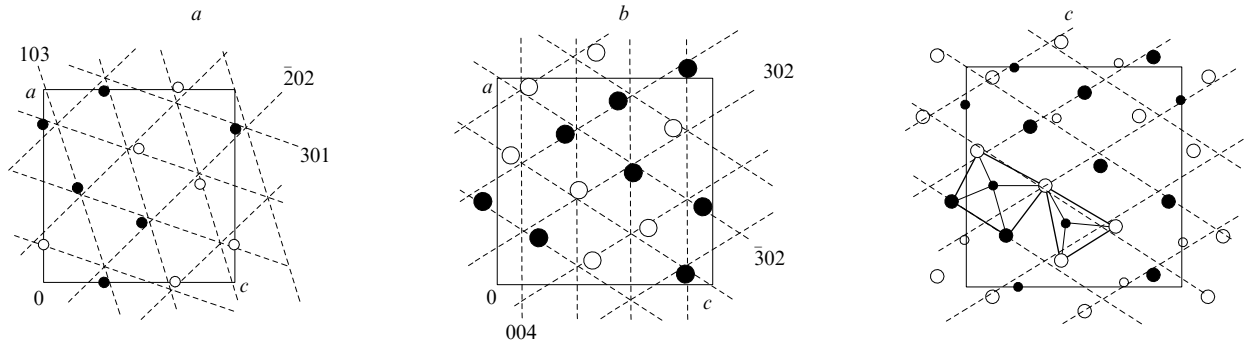


Figure 8. Structure of Tm_2S_3.
The cation (*a*) and anion (*b*) positions projected along the *b* axis [16] and the networks of cation and anion sublattice points at two heights. Empty and filled circles correspond to atomic positions on mirror planes at $y = 1/4$ and $y = 3/4$, respectively; projections of cations (small circles) and anions (large circles) onto the *xz* plane. Trigonal prisms formed by sulfur anions around two basis Tm atoms, with their trigonal faces resting upon the *xz* plane and those lying on the edge.

anion sublattice provides the coordination environment of two basis atoms located in the centres of trigonal prisms in two orientations, with their triangular faces resting upon the *xz* plane and those lying on the edge. The example of Tm_2S_3 shows the difficulties in assembling the structure even through two mechanisms of ordering: the sublattices should be commensurate, *i.e.*, an integer number of the nodes of one sublattice and an integer number of the nodes of another one (in the general case, another number) should be present in the translational unit cell, and the atoms should have the coordination in the first sphere admissible for these atoms. The presence of vacant nodes in sublattices and the possibility of small deviations of atomic positions from the nodes are responsible for the formation of stable structures. Therefore, a particular crystal structure represents a compromise between the chemical forces providing the short-range order due to interatomic interactions and the forces creating the long-range order, *i.e.*, mechanical forces of elastic vibrations (according to the mechanical-wave concept).[28,35]

IV.1. Sulfides with the arrangement of atomic positions as in sphalerite and galena

As mentioned above, natural and synthetic sulfides crystallize mainly in the cubic sphalerite[16,36–55] and galena[56–58] structure types with the cation : anion ratio equal to 1 : 1. Data on numerous compounds having such structures are available in monographs on structures of inorganic compounds[36] and reviews on sulfides.[30,31] In these structures, the skeletal planes of cation and anion sublattices are the planes of {111} families with trigonal planar networks of atoms arranged according to the simplest cubic close packing (ABC type) perpendicular to the body diagonal of the cubic unit cell, as well as the coordinate planes (200), (020) and (002) of the *F* unit cell with square nets.

The goal of crystallographic analysis is to follow the changes in the atomic configurations caused by deviations from the ideal stoichiometric cation : anion ratio and to establish the factors responsible for the reduction of the symmetry. The structures of the minerals aktashite, galkhaite, stalderite and As-schwatzite with atomic positions arranged according to the sphalerite lattice were analyzed.[16,37–42] In the trigonal structure of aktashite $Cu_6Hg_3As_4S_{12}$,[43,44] the rhombohedral subcell is very similar to the cubic unit cell, and the $(\bar{1}41)$, $(\bar{3}\bar{1}1)$ and $(4\bar{3}1)$ planes, which are related by a symmetry axis and correspond to the {111}-type planes of the pseudotranslational cubic unit cell, were found to be the skeletal planes with the maximum density of both cations and anions. The (312), $(\bar{4}32)$ and $(1\bar{4}2)$ planes related by a three-fold axis are the {200}-type coordinate planes for the *F*-subcell, and these planes determine the parameters of the pseudocubic *F*-sublattice (Tables 7 and 8).

Table 7. Crystallographic data for $Cu_6Hg_3As_4S_{12}$, $(Hg,Cu,Zn)_{12}(Cs,Tl)_2As_8S_{24}$, $AgHgAsS_3$ and Hg_3SbAsS_3.

$Cu_6Hg_3As_4S_{12}$ (space group *R*3) (Refs 14, 43)	$(Hg,Cu,Zn)_{12}(Cs,Tl)_2As_8S_{24}$ (space group $I\bar{4}3m$) (Ref. 49)	$AgHgAsS_3$ (space group *Aa*) (Ref. 57)	Hg_3SbAsS_3 (space group $P2_1/n$) (Ref. 16)
Unit cell parameters:	Unit cell parameters:	Unit cell parameters:	Unit cell parameters:
$a = 13.780$, $c = 9.329$,	$a = 10.379$,	$a = 7.732$, $b = 11.285$, $c = 6.643$,	$a = 11.552$, $b = 4.385$, $c = 15.673$,
$Z = 3$, $N = 39/36$ (see [a]),	$Z = 1$, $N = 22/24$,	$\beta = 115$, $Z = 4$, $N = 12/12$,	$\beta = 91.84$, $Z = 4$, $N = 16/16$,
$V_c/V_0 = 4/39$	$V_c/V_0 = 1/8$	$V_c/V_0 = 1/3$	$V_c/V_0 = 1/4$
Transformation matrix to the subcell:	Transformation matrix to the subcell:	Transformation matrix to the subcell:	Transformation matrix to the subcell:
14/39 10/39 1/3	1/2 0 0	1/2 −1/3 0	1/2 0 0
−10/39 4/39 1/3	0 1/2 0	1/2 1/3 0	0 1 −1/4
−4/39 −14/39 1/3	0 0 1/2	1/2 0 1	0 1 1/4
Parameters of the cation subcell:	Parameters of the cation subcell:	Parameters of the cation subcell:	Parameters of the cation subcell:
$a_c = b_c = c_c = 5.40$,	$a_c = b_c = c_c = 5.19$,	$a_c = b_c = 5.394$, $c_c = 6.102$,	$a_c = 5.78$, $b_c = c_c = 5.88$,
$\alpha_c = \beta_c = \gamma_c = 90.13$	$\alpha_c = \beta_c = \gamma_c = 90$	$\alpha_c = \beta_c = 82.97$, $\gamma_c = 88.44$	$\alpha_c = 96.57$, $\beta_c = \gamma_c = 91.23$

[a] *N* is the cation to anion ratio in the unit cell.

Table 8. Results of crystallographic analysis of the $Cu_6Hg_3As_4S_{12}$, $(Hg,Cu,Zn)_{12}(Cs,Tl)_2As_8S_{24}$, $AgHgAsS_3$ and Hg_3SbAsS_3 structures.

$Cu_6Hg_3As_4S_{12}$ (Refs 14, 43)					$(Hg,Cu,Zn)_{12}(Cs,Tl)_2As_8S_{24}$ (Ref. 49)					$AgHgAsS_3$ (Ref. 57)					Hg_3SbAsS_3 (Ref. 16)				
hkl	d_{hkl}	$(\rho_{hkl})_c$	$(\rho_{hkl})_a$	$(hkl)_c$, $(hkl)_a$	*hkl*	d_{hkl}	$F_c > 600$	$F_a > 100$	$(hkl)_c$, $(hkl)_a$	*hkl*	d_{hkl}	$(\rho_{hkl})_c$	$(\rho_{hkl})_a$	$(hkl)_c$, $(hkl)_a$	*hkl*	d_{hkl}	$(\rho_{hkl})_c$	$(\rho_{hkl})_a$	$(hkl)_c$, $(hkl)_a$
003	3.12	0.98	0.94	111	222	3.00	809	252	111	200	3.508	0.97	0.94	111	210	3.492	0.90	–	111
$\bar{1}41$				111	004	2.60	908	225	002	031	3.201	0.93	0.78	$\bar{1}11$	$\bar{2}04$	3.285	0.95	0.82	$\bar{1}\bar{1}1$
$\bar{3}\bar{1}1$	3.11	0.96	0.96	$\bar{1}11$	044	1.84	818	153	022	002	3.014	0.99	0.93	002	204	3.188	0.97	0.89	$1\bar{1}1$
$4\bar{3}1$				$1\bar{1}1$	226	1.57	666	120	113	$\bar{2}02$	3.006	1.00	0.96	$11\bar{1}$	014	2.917	0.89	0.61	002
312				200	444	1.50	756	110	222	$\bar{2}31$	2.687	0.93	0.77	200	400	2.886	0.95	0.74	200
$\bar{4}32$	2.69	0.95	0.95	020						231	2.136	0.89	0.71	022	020	2.193	0.68	–	022
$1\bar{4}2$				002						202	1.918	0.93	0.79	113	$\bar{4}14$	2.077	0.82	–	$\bar{2}02$
										$\bar{4}02$	1.911	0.96	0.89	220	414	2.028	0.86	–	202
										$\bar{2}33$	1.897	0.94	0.73	$\bar{2}02$					

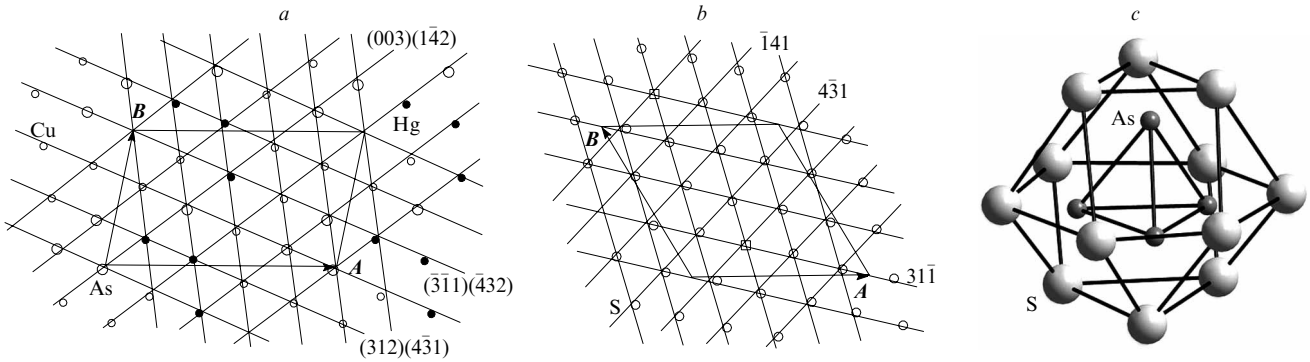


Figure 9. Structure of $Cu_6Hg_3As_4S_{12}$.[43]
(*a*) A trigonal (3^6) network of cations in the ($\bar{1}41$) plane formed by the traces of the cross-sections by other close-packed planes; the translations of the plane unit cell: $\boldsymbol{A} = \boldsymbol{a} - \boldsymbol{c} = 16.635$ Å, $\boldsymbol{B} = -2/3\,\boldsymbol{a} - 1/3\,\boldsymbol{b} + 2/3\,\boldsymbol{c} = 10.096$ Å, $\gamma = 77.58°$; (*b*) a trigonal (3^6) network of anions in the (003) plane formed by the traces of the cross-sections by other close-packed planes; the translations of the plane unit cell: $\boldsymbol{A} = \boldsymbol{b}$, $\boldsymbol{B} = \boldsymbol{a}$, □ is a vacant lattice point; (*c*) the building block of $[As_4S_{12}]^{12-}$ is the empty $[As_4]^{12+}$ tetrahedron surrounded by sulfur atoms at the vertices of a cuboctahedron.

In the unit cell of the hexagonal structure of aktashite, there are 39 lattice points accessible for filling both in the cation and anion subcells. In the cation subcell, all lattice points are occupied by three types of cations, *viz*., copper, mercury and arsenic (Fig. 9 *a*). In the anion subcell, which is analogous to the cation subcell but is shifted with respect to the latter, three nodes on three-fold axes remain vacant (Fig. 9 *b*). This gives rise to building block characteristic of the aktashite structure, namely, the empty $[As_4]^{12+}$ tetrahedron with the distances As–As = 3.514–3.576 Å, which is surrounded by sulfur atoms occupying the vertices of the cuboctahedron (Fig. 9 *c*). Of a rich set of symmetry elements available in the sphalerite structure type, only one three-fold axis exists in the case under consideration. This is not surprising taking into account that the structure contains three, rather than one, types of cations in the 6 : 3 : 4 ratio. Nevertheless, the complex of close-packed atomic planes and their mutual orientation (see Table 8) remain almost the same as in the ideal sphalerite structure, and the sulfur atoms are also distributed over the nodes of the ideal anion sublattice with strictly localized vacancies, *i.e*., it is commensurate with the cation sublattice, as required for the 1 : 1 ratio.

In the cubic structure of the mineral galkhaite $(Hg,Cu,Zn)_{12}(Cs,Tl)_2As_8S_{24}$,[45–49] there are eight sphalerite cells with the parameter $a_c = a/2 \approx 5.19$ Å per unit cell (see Tables 7 and 8), and the latter should include $4 \times 8 = 32$ both cation and anion positions. In fact, the cation subcell contains 20 cations [12 (Hg,Cu,Zn) + 8 As] and 24 anions. The distribution of 12 vacant lattice points in the cation sublattice is not uniform, and these vacancies are arranged in two octahedra with the centres in the origin of the coordinates and in the centre of the *I* unit cell of the structure, respectively. Eight vacant lattice points in the anion sublattice form two tetrahedra with the centres at the same (000) and (1/2 1/2 1/2) sites. The resulting void is occupied by a large monovalent (Cs,Tl) cation surrounded by 12 sulfur anions. This cation, apparently, stabilizes the structure but occupies the unusual position with respect to the lattice points in the cation matrix. The distribution of cations, anions and vacancies in the (222) planes is shown in Fig. 10.

The arrangement of cations and anions similar to that in the galkhaite structure was found in the tetragonal structure of stalderite $TlCu(Zn,Fe,Hg)_2As_2S_6$ (space group $I\bar{4}2m$,

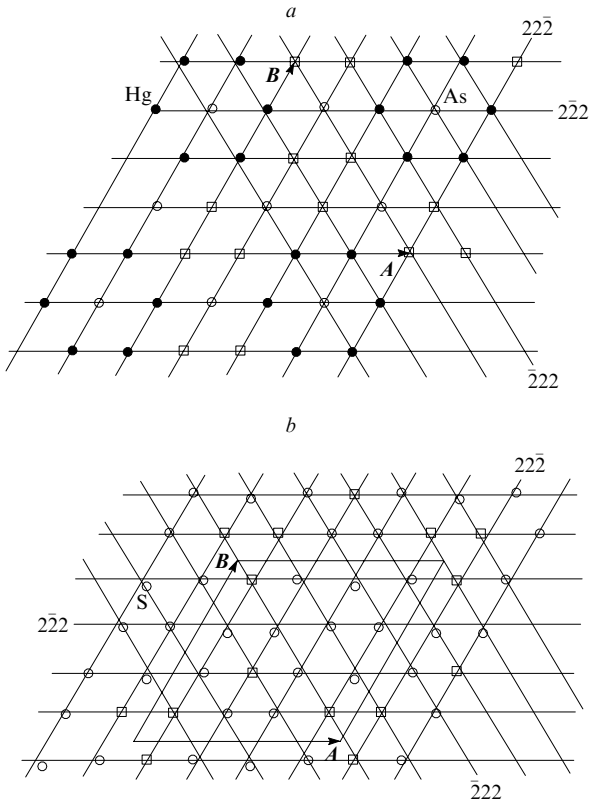


Figure 10. Structure of galkhaite $(Hg,Cu,Zn)_{12}(Cs,Tl)_2As_8S_{24}$.[49]
(*a*) A network of lattice points in the (222) plane formed by its cross-sections by the (2$\bar{2}$2), (22$\bar{2}$) and ($\bar{2}$22) planes and the real positions of Hg and As cations; □ are vacant lattice points; $\boldsymbol{A}$ and $\boldsymbol{B}$ are translations in this plane (and the angle between these translations) $\boldsymbol{A} = -\boldsymbol{a} + \boldsymbol{c} = 14.658$ Å, $\boldsymbol{B} = -\boldsymbol{a} + \boldsymbol{b} = 14.658$ Å; $\gamma = 60°$; (*b*) an analogous network of lattice points shifted with respect to the previous one; the real positions of sulfur atoms on the (222) plane.

$Z = 4$, $a = 9.855$ Å, $c = 10.937$ Å).[50, 51] In this structure, large voids with the centres at (000) and (1/2 1/2 1/2) are occupied by pairs of monovalent thallium cations (Tl–Tl = 3.29 Å). The $[Tl_2]$ dumbbell pair oriented along the *c* axis is responsible for the tetragonal distortion of the

cubic cation and anion skeletons of the structure. Stalderite is isostructural with $Tl(Cu,Ag)(Hg,Zn)_2(As,Sb)_2S_6$, routhierite,[51] which has a somewhat different cation composition.

Another variant of the sphalerite structure type is observed in $Cu_6(Cu_{5.25}Hg_{0.75})(As_{2.83}Sb_{1.17})S_{13}$, As-schwatzite (space group $I\bar{4}3m$, $Z = 2$, $a = 10.289$ Å).[52–54] There are 32 cations per eight sphalerite subcells in the unit cell of this structure, *i.e.*, all positions in the cation framework are occupied. By contrast, anions, like those in the galkhaite structure, leave vacant two tetrahedra with the centres at (000) and (1/2 1/2 1/2), and they are occupied by 'non-standard' sulfur anions. The replacement of four anions by one anion substantially changes the coordination of the octahedral group consisting of six copper cations and centred by the so-called thirteenth sulfur atom.[30] The unusual triangular coordination of six copper cations sharing a vertex occupied by this anion is illustrated in Fig. 11.

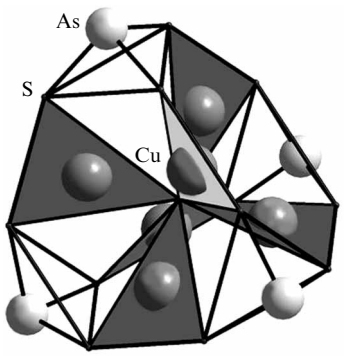


Figure 11. Structure of schwatzite $Cu_6(Cu_{5.25}Hg_{0.75})(As_{2.83}Sb_{1.17})S_{13}$: the unusual triangular coordination of six copper cations sharing a vertex occupied by a sulfur anion.[54]

The above examples demonstrate high stability of symmetric cation and anion 'skeletons' of the sphalerite structure type formed by families of close-packed planes with trigonal atomic networks intersecting each other at angles determined by symmetry operations. A high percentage of vacant lattice points (up to ~40%), the inclusion of atoms in interstitial positions, anomalous coordination, *etc.*, are admissible. It should be noted that in all cases, the cation and anion frameworks are commensurate, which corresponds to the 1 : 1 stoichiometry of the lattice points.

Stability of these configurations is confirmed by the fact that all of them are inherent in the structures of another composition. For instance, the cation framework of aktashite is replicated in the structure of fluoride $K_7Th_6F_{31}$ (space group $R\bar{3}$, Z = 3, $a = 15.293$ Å, $c = 10.449$ Å),[20] and the analogue of the cation framework of galkhaite is observed in the structure of $TR_3Sb_5O_{12}$ (space group $I\bar{4}3m$, $Z = 2$, $a = 10.743$ Å for TR = Y).[55]

As mentioned above, the mutual displacement of the cubic cation and anion sublattices by one-half of the diagonal (or the edge) of the *F* unit cell results in that the cations and anions are in the mutual octahedral environment, thus extending the range of chemical compositions for the crystallization in the galena structure type.

The crystallographic analysis of monoclinic laffittite $AgHgAsS_3$ with the cation : anion stoichiometry of 1 : 1 was performed.[56, 57] Figure 12 presents the arrangement of cations and anions in the crystallographic (031) planes corresponding to the {111} planes for the cation and anion *F*-subcells shifted with respect to each other (see Tables 7 and 8). In each unit cell, the arrangement of the atoms is quite regular, but their mutual arrangement deviates from the ideal geometry, as can be seen in Fig. 12*c*, where the square networks of cations and anions in the coordinate planes of *F*-subcells should centre each other; however, in reality the deviation from this condition takes place due to anisotropy of the As–S and Hg–S chemical bonds. The geometric characteristics of the real *F*-subcell of atoms substantially differ from those of the ideal cubic unit cell (see Table 7). The translational unit cell of the structure comprises three *F*-subcells.

The mineral tvalchrelidzeite Hg_3SbAsS_3,[58] which contains As^{3-} and S^{2-} anions and, consequently, has the cation : anion stoichiometry of 1 : 1, is another example of structures having a sublattice of the galena type. Data on the characteristics of the sublattices and 'skeletal' planes for the cation and anion sublattices are given in Tables 7 and 8. The real distribution of Hg^{2+} and Sb^{3+} cations is more regular, and their positions almost exactly coincide with the sublattice points, as can be seen from the atomic positions in the (014) plane serving as the coordinate plane of the *F*-sublattice (Fig. 13*a*). Another coordinate plane of the *F*-sublattice (Fig. 13*b*) includes, along with the cation positions, the positions of As^{3-} and S^{2-} anions character-

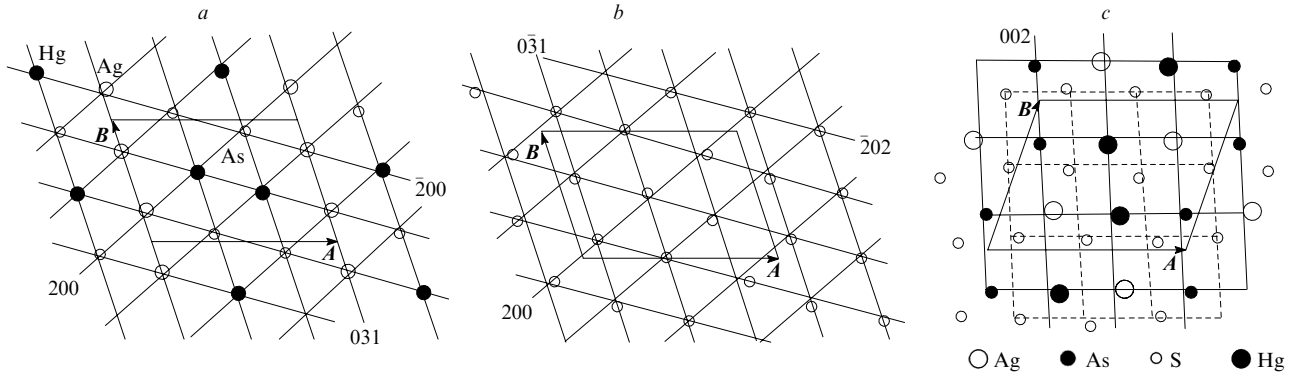


Figure 12. Structure of laffittite $AgHgAsS_3$.[57]
(*a*) The cation network 3^6 in the (031) plane and the traces of its cross-sections by the (200), ($\bar{2}02$) and ($0\bar{3}1$) planes; (*b*) the related anion network 3^6 in the (031) plane and the traces of its cross-sections by the (200), ($\bar{2}02$) and ($0\bar{3}1$) planes: $\boldsymbol{A} = \boldsymbol{a} - 1/2\,\boldsymbol{b} - 3/2\,\boldsymbol{c} = 11.23$ Å, $\boldsymbol{B} = -\boldsymbol{a} = 7.756$ Å, $\gamma = 108.13°$; (*c*) quasisquare networks of silver, mercury and arsenic cations and the related sulfur anion networks in the ($\bar{2}31$) plane. $\boldsymbol{A} = -1/2\,\boldsymbol{b} + 3/2\,\boldsymbol{c} = 11.492$ Å, $\boldsymbol{B} = -\boldsymbol{a} - 1/2\,\boldsymbol{b} - 1/2\,\boldsymbol{c} = 9.019$ Å, $\gamma = 72.10°$.

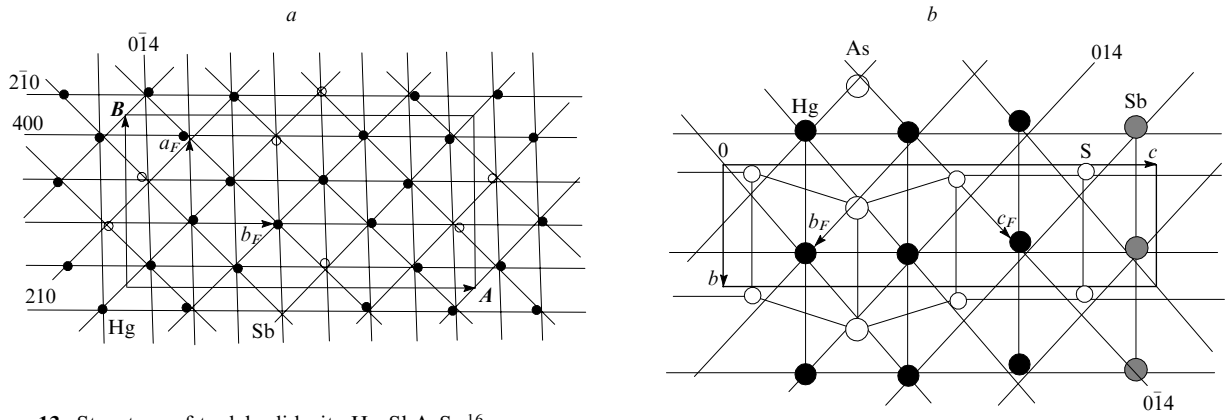


Figure 13. Structure of tvalchrelidzeite Hg_3SbAsS_3.[16]
(*a*) Hg and Sb cations in the (014) plane; $\boldsymbol{A} = -4\boldsymbol{b} + \boldsymbol{c}$ = 23.498 Å, $\boldsymbol{B} = \boldsymbol{a}$ = 11.552 Å, γ = 91.23°, traces of the cross-sections by the (210), (2$\bar{1}$0), (400) and (0$\bar{1}$4) planes; (*b*) quasisquare networks of (Hg, Sb) cations and networks of (As, S) anions in the (400) plane. The traces of the cross-sections of this plane by the close-packed (014) and (0$\bar{1}$4) planes.

ized by a less regular distribution. The monoclinic (but pseudoorthorhombic) unit cell of the Hg_3SbAsS_3 structure comprises four *F*-subcells, in which all lattice points are occupied by both cations and anions.

A comparison of the structures of sphalerite and galena types showed that the former are more regular and more symmetric, the deviations from the standard geometry being relatively small. This can be attributed to stronger chemical bonds between atoms in the case of their mutual tetrahedral environment in the sphalerite structure type compared to the octahedral environment in the galena structure type.

IV.2. Lozenge-shaped sulfides

Structures with a short (~4 Å) translation and a mirror plane perpendicular to this translation are often found among natural and synthetic sulfides. Additional mirror planes that arise in these structures give rise to families of crystallographic planes with $d_{hkl} \approx 2$ Å. Since the mirror plane requires that the centre of the atom be either in this plane or at a distance larger than the atomic radius from this plane, all atoms in these structures have to be located only on mirror planes.

The frequent repetition of the short translation can be attributed to the fact that the diameter of the sulfur anion (generally, the largest atom in the structure) is of the same order; consequently, all these structures consist of not more than two independent or symmetry-related atomic layers. For the above-mentioned reason, the mirror planes are ideal 'regulators' of atomic positions, since the centres of the atoms are concentrated in these planes.

Even for relatively simple compositions, the unit cell having one short translation (~4 Å) will have relatively large two other translations, *i.e.*, it will resemble a platelet, accounting for the name of these structures. The translations on mirror planes are as long as ~100 Å.

It is reasonable to use the atomic network coinciding with the mirror plane as the coordinate plane in the calculations of cation and anion subcells, although the absolute atomic density of this plane may be lower compared to other planes due to the necessary presence of vacant lattice points. As was shown for the Tm_2S_3 structure, the short translation of the sublattice perpendicular to the mirror plane (~2.0 Å) requires the alternation of occupied and vacant lattice points. Let us illustrate this situation using the relatively simple Tm_5S_7 structure (Table 9),[34] which has the following characteristics:

— the unit cell parameters: a = 12.455, b = 3.740, c = 11.268, β = 105.4, Z = 2, N = 10/14;

— the transformation matrix to the cation subcell:

$$\begin{matrix} 3/10 & 0 & 2/10 \\ 0 & 1/2 & 0 \\ -2/10 & 0 & 2/10 \end{matrix}$$

— the transformation matrix to the anion subcell:

$$\begin{matrix} 3/14 & 0 & -1/7 \\ 0 & 1/2 & 0 \\ 1/14 & 0 & 4/14 \end{matrix}$$

— the parameters of the cation sublattice: a_c = 3.82, b_c = 1.87, c_c = 3.78, α_c = 90, β_c = 110.2, γ_c = 90, V_c/V_0 = 1/20;

— the parameters of the anion sublattice: a_a = 3.46, b_a = 1.87, c_a = 3.10, α_a = 90, β_a = 115.96, γ_a = 90, V_a/V_0 = 1/28.

The results of the crystallographic analysis of Tm_5S_7 are presented in Table 9. Figure 14 shows the cation and anion positions projected along the short axis b = 3.74 Å. The (202) and (2$\bar{0}$3) planes are the coordinate planes of the cation sublattice perpendicular to the projection; for the

Table 9. Relative densities of filling with atoms (ρ) of the crystallographic planes (*hkl*) most close-packed by cations and anions; interplanar spacings d_{hkl} and indices in the sublattices of the Tm_5S_7 structure.[34]

hkl	d_{hkl}	$(\rho_{hkl})_c$(> 0.9)	$(hkl)_c$	*hkl*	d_{hkl}	$(\rho_{hkl})_a$(> 0.6)	$(hkl)_a$
202	3.58	0.96	100	401	3.11	0.76	100
203	3.54	0.98	001	402	2.98	0.62	–
401	3.11	0.99	101	203	2.79	0.95	001
005	2.17	0.98	101	204	2.77	0.87	101
601	1.88	0.91	201	601	1.88	0.77	–
020	1.87	1.00	010	020	1.87	1.00	010

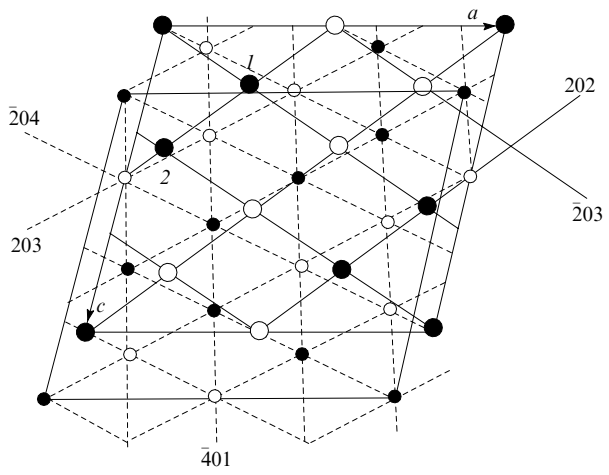


Figure 14. Structure of Tm_5S_7 projected along the *b* axis.[16]
Solid lines indicate the sublattice of thulium cations represented by large circles (empty and filled circles, respectively, at $y = 0$ and $y = 1/2$), dashed lines indicate the sublattice of anions (small circles at $y = 0$ and $y = 1/2$). *1*, Tm in the [6S] prism; *2*, Tm in the [6S] octahedron.

anion sublattice, such planes are ($\bar{4}01$) and (203). In the unit cell, the total number of lattice points in the cation sublattice $\det\{202/020/\bar{2}03\} = 20$; in the anion sublattice, $\det\{203/020/\bar{4}01\} = 28$, *i.e.*, in both sublattices, all positions accessible for filling are occupied. Taking into account that there are two atomic layers in this projection of the structure, it is evident that one of the basis thulium atoms is coordinated in the centre of the trigonal prism formed by sulfur atoms (the triangular face on the *xz* plane), whereas another thulium atom is located in the centre of an octahedron, with its square section being perpendicular to the *xz* plane.

Since the cation : anion ratio in the structure is 5 : 7, and the sublattice points are occupied, the sublattices are incommensurate, as can be seen from the values of these translations. The mirror planes are responsible for the equality of the translations b_c and b_a, but a_c and c_c are substantially longer than a_a and c_a.

As follows from the analysis of the crystal-chemical data, the structure contains PbS-type fragments, with the cations being in an octahedral coordination. However, there is also another coordination that is formed due the necessity of accommodation of 'independent' cation and anion orderings by different systems of parallel planes in the course of crystallization. The formation of incommensurate pseudotranslational subcells for different groups of atoms is evidence of the existence of long-range forces responsible for the appearance of the crystalline state as a result of the ordering of atomic positions taking into account, to the maximum extent, the short-range order due to interatomic interactions (chemical bonds).

The above-considered crystallographic analysis technique as applied to the relatively simple structure is typical of lozenge-shaped sulfides and just of them. The cation framework with a pseudohexagonal subcell (one-half of lattice points is occupied) found in the structure can be referred to as a unified skeleton of these compounds and their, so to say, common genome. Depending on the composition, the cation distribution over cation sublattice points is individual for each structure, and it is reasonable to use this feature for the description and classification by determining the degree of similarity.

The anion configuration (anion framework) is less specific because of the uniformity of the composition, although sulfur atoms in natural compounds can be partially replaced by oxygen, selenium and tellurium atoms. In the structures studied by our research team, the parameters of anion sublattices vary in wider ranges and the filling densities of the skeletal planes are usually lower than those of the cation sublattices. This fact indicates that anion sublattices play a minor role in the structure formation.

The results of crystallographic analysis[37–39,42,59–67] and X-ray diffraction data[68–103] for the structures assigned to lozenge type are summarized in Table 10.

The presence of a short translation in lozenge-shaped structures of sulfides makes the crystal chemical analysis much easier. Thus in this direction, all types of coordination polyhedra are linked *via* either shared faces or edges to form columns or ribbons, respectively. The modular analysis is developed mainly for such structures.[32,33] According to this method, the structures are divided into blocks having structures of sphalerite, galena, *etc.* types. Let us consider the application of this technique for the complex structure of cupromakopavonite $Cu_8Ag_3Pb_4Bi_{19}S_{38}$ (see Table 10). Figure 15 presents the projections of cations along the short *b* axis and networks of lattice points of the cation and anion skeletons. In the cation skeleton, the number of sublattice points, which can be occupied, is smaller than the number of cations and, in order to overcome this problem (like in some other structures), small Cu^+ cations are located in close proximity to the chain of lattice points along the *b* axis located at a short distance of 2 Å. In this case, the Cu–Cu distance decreases to 2.84 Å. Although copper cations substantially deviate from the chain of sublattice points, this does not cause distortions in the regular arrangement of positions of other cations. There are no substantial distortions in the anion skeleton (see Fig. 15 *b*). In Fig. 15 *c*, both frameworks are superimposed, and it can be seen that most of cations are in octahedral environment formed by sulfur atoms (*i.e.*, the galena structure type is reproduced); however, the layers of these octahedra in the *xy* plane are separated in the unit cell by two layers of columns of Pb prisms sharing triangular faces in the *xz* plane. These layers are adjoined by copper cations in a three-fold coordination rare for these atoms.[104]

The $Cu_8Ag_3Pb_4Bi_{19}S_{38}$ structure provides additional evidence of stability of the cation and anion frameworks that are formed due to the three-dimensional ordering of the positions of the basis (including heavy) atoms. This is an example of structures characterized by inconsistency between the composition and the framework.

An analysis of the parameters of the cation and anion sublattices in the structures of lozenge-shaped sulfides (see Table 10) showed that they are similar to a certain standard — the pseudohexagonal sublattice with the translations a_c, c_c within $\sim 4.1 \pm 0$ Å, a_a, c_a within $\sim 3.6 \pm 0.5$ Å at b_c, $b_a \sim 2.0 \pm 0.1$ Å and the angles β_c, β_a of $\sim 120^\circ$. A similar configuration can be seen in the cubic galena structure type after the transformation from the *F*-unit cell to the tetragonal *I*-unit cell when considering the projection of the structure onto the (220) diagonal plane (Fig. 16 *a*,*b*). Two networks of lattice points, which coincide with the mirror planes perpendicular to the translation that centres the face of the *F*-unit cell [it is equal to ~ 4 Å ($a_F\sqrt{2}/2$)], reproduce typical cation and anion frameworks of lozenge-shaped

Table 10. Results of crystallographic analysis and X-ray diffraction data for lozenge-shaped structures of sulfides.

Unit cell parameters	Skeletal planes of *hkl* su blattices	Number of lattice points per unit cell	Parameters of the cation and anion subcells	Ref.
Marrucciite $Hg_3Pb_{16}Sb_{18}S_{46}$ (space group $C2/m$, $Z = 2$, $N = 74/92$)				
$a = 48.124$, $b = 4.1083$,	for cations: 803, $\bar{6}07$, 020	148	$a_c = 4.00$, $b_c = 3.92$, $c_c = 2.05$, $\gamma_c = 119.35$	38, 39,
$c = 23.990$, $\beta = 118.76$	for anions: $160\bar{3}$, 1004, 020	188	$a_a = 3.61$, $b_a = 3.98$, $c_a = 2.06$, $\gamma_a = 131.2$	67, 68
Livingstonite $HgSb_4S_8$ (space group $A2/a$, $Z = 8$, $N = 40/64$)				
$a = 30.154$, $b = 3.995$,	for cations: $\bar{8}02$, 020, $40\bar{6}$	80	$a_c = 4.50$, $b_c = 4.18$, $c_c = 1.99$, $\gamma_c \approx 124$	59, 62,
$c = 21.426$, $\beta = 104.26$	for anions: 406, 020, $\bar{4}08$	112	$a_a = 4.20$, $b_a = 3.90$, $c_a = 1.99$, $\gamma_a \approx 137$	70, 71
Kupcikite $(Cu,Fe)_4Bi_5S_{10}$ (space group $C2/m$, $Z = 2$, $N = 18/20$)				
$a = 17.512$, $b = 3.9103$,	for cations: $\bar{2}04$, 401, 020	36	$a_c = 3.69$, $b_c = 1.96$, $c_c = 3.19$, $\beta_c = 104.68$	59, 72
$c = 12.869$, $\beta = 108.56$	for anions: $\bar{2}04$, 402, 020	40	$a_a = 3.32$, $b_a = 1.96$, $c_a = 3.46$, $\beta_a = 116.6$	
Felbertalite $Cu_2Pb_6Bi_2S_{19}$ (space group $C2/m$, $Z = 2$, $N = 20/38$)				
$a = 27.64$, $b = 4.05$,	for cations: $\bar{8}03$, 203, 020	60	$a_c = 3.82$, $b_c = 4.25$, $c_c = 2.03$, $\gamma_c = 117.78$	59, 67,
$c = 20.74$, $\beta = 131.26$	for anions: $\bar{8}03$, 204, 020	76	$a_a = 3.72$, $b_a = 3.36$, $c_a = 2.03$, $\gamma_a = 114.74$	73
Kudriavite $(Cd,Pb)Bi_2S_4$ (space group $C2/m$, $Z = 4$, $N = 12/16$)				
$a = 13.095$, $b = 4.003$,	for cations: $\bar{2}04$, 202, 020	24	$a_c = 3.92$, $b_c = 3.98$, $c_c = 2.01$, $\gamma_c = 111.92$	60, 62,
$c = 14.711$, $\beta = 115.59$	for anions: $\bar{2}05$, 203, 020	32	$a_a = 3.69$, $b_a = 3.65$, $c_a = 2.01$, $\gamma_a = 126.26$	74
$Bi_2In_4S_9$ (space group $P2_1/m$, $Z = 2$, $N = 12/18$)				
$a = 16.167$, $b = 3.917$,	for cations: $\bar{4}02$, 401, 020	24	$a_c = 4.03$, $b_c = 4.42$, $c_c = 1.96$, $\gamma_c = 123.10$	60, 62,
$c = 11.111$, $\beta = 94.04$	for anions: $\bar{6}02$, 601, 020	36	$a_a = 3.87$, $b_a = 4.00$, $c_a = 1.96$, $\gamma_a = 140$	75
$Bi_3In_5S_{12}$ (space group $C2/m$, $Z = 4$, $N = 32/48$)				
$a = 33.13$, $b = 3.873$,	for cations: $\bar{8}02$, 004, 020	64	$a_c = 4.14$, $b_c = 1.94$, $c_c = 4.12$, $\gamma_c = 118.97$	60, 62,
$c = 14.413$, $\beta = 91.21$	for anions: 005, 1002, 020	100	$a_a = 3.31$, $b_a = 3.20$, $c_a = 1.94$, $\gamma_a = 115.69$	76
$Pb_4In_2Bi_4S_{13}$ (space group $Pbam$, $Z = 4$, $N = 40/52$)				
$a = 21.344$, $b = 26.494$,	for cations: $\bar{6}01$, $\bar{4}60$, 020	40	$a_c = 4.16$, $b_c = 4.01$, $c_c = 2.00$, $\gamma_c = 122$	60, 62,
$c = 4.002$	for anions: 570, 800, 002	56	$a_a = 3.78$, $b_a = 3.57$, $c_a = 2.00$, $\gamma_a = 134$	77
$Pb_4In_3Bi_7S_{18}$ (space group $P2_1/m$, $Z = 2$, $N = 28/36$)				
$a = 21.021$, $b = 4.014$,	for cations: $\bar{6}01$, $\bar{3}05$, 020	54	$a_c = 4.19$, $b_c = 4.18$, $c_c = 2.00$, $\gamma_c = 123.42$	60, 62,
$c = 18.898$, $\beta = 97.07$	for anions: $\bar{6}01$, $\bar{4}06$, 020	64	$a_a = 4.34$, $b_a = 3.52$, $c_a = 2.00$, $\gamma_a = 126.30$	78
$Pb_{1.6}In_8Bi_4S_{19}$ (space group $C2/m$, $Z = 2$, $N = 30.4/38$)				
$a = 29.167$, $b = 3.872$,	for cations: $\bar{8}03$, 601, 020	52	$a_c = 4.29$, $b_c = 4.17$, $c_c = 1.94$, $\gamma_c = 123.6$	60, 79
$c = 15.554$, $\beta = 121.6$	for anions: $\bar{2}05$, 801, 020	84	$a_a = 3.38$, $b_a = 3.15$, $c_a = 1.94$, $\gamma_a = 120.12$	
Lillianite $Pb_3Bi_2S_6$ (space group $Bbmm$, $Z = 4$, $N = 20/24$)				
$a = 13.540$, $b = 20.637$,	for cations: 002, 250, $\bar{2}50$	40	$a_c = b_c = 3.96$, $c_c = 2.06$, $\gamma_c = 117.26$	63, 80
$c = 4.1103$	for anions: 260, $\bar{2}60$, 002	64	$a_a = b_a = 3.80$, $c_a = 2.06$, $\gamma_a = 126.13$	
β-Lillianite $Pb_3Bi_2S_6$ (space group $Pbnm$, $Z = 4$, $N = 20/24$)				
$a = 11.026$, $b = 23.023$,	for cations: 310, 170, 002	40	$a_c = 4.03$, $b_c = 3.50$, $c_c = 2.01$, $\gamma_c = 115.68$	63, 81
$c = 4.023$	for anions: 270, $\bar{2}70$, 002	28	$a_a = 3.21$, $b_a = 3.21$, $c_a = 2.06$, $\gamma_a = 118.36$	
Heyrovskyite $Pb_6Bi_2S_9$ (space group $Pbmm$, $Z = 4$, $N = 32/36$)				
$a = 13.794$, $b = 31.393$,	for cations: 028, $0\bar{2}8$, 200	64	$a_c = b_c = 3.96$, $c_c = 2.01$, $\gamma_c = 120.37$	63, 81,
$c = 4.1319$	for anions: 029, $0\bar{2}9$, 200	36	$a_a = b_a = 3.86$, $c_a = 2.07$, $\gamma_a = 126.01$	82
Cannizzarite $(Pb,Cd)_5(Bi,In)_6(S,Se)_{14}$ (space group $P2_1/m$, $Z = 2$, $N = 22/28$)				
$a = 15.417$, $b = 4.058$,	for cations: 400, $\bar{2}06$, 020	48	$a_c = 4.00$, $b_c = 3.47$, $c_c = 2.03$, $\gamma_c = 107.39$	83–85
$c = 20.807$, $\beta = 98.03$	for anions: 500, $\bar{2}06$, 020	60	$a_a = 3.20$, $b_a = 3.47$, $c_a = 2.03$, $\gamma_a = 107.39$	
Moëloite $Pb_6Sb_6S_{14}(S_3)$ (space group $P2_122_1$, $Z = 2$, $N = 24/30$)				
$a = 15.328$, $b = 4.04$,	for cations: 403, $40\bar{3}$, 020	48	$a_c = 4.29$, $b_c = 4.29$, $c_c = 2.02$, $\gamma_c = 126.99$	86, 87
$c = 23.054$	for anions: 503, $50\bar{3}$, 020	60	$a_a = b_a = 4.14$, $c_a = 2.0$, $\gamma_a = 136.50$	

Table 10 (continued).

Unit cell parameters	Skeletal planes of *hkl* sublattices	Number of lattice points per unit cell	Parameters of the cation and anion subcells	Ref.
$Pb_4In_9S_{17}$ (space group *Pbam*, $Z = 2$, $N = 26/34$)				
$a = 22.761$, $b = 15.201$, $c = 3.858$	for cations: 340, $\bar{3}40$, 002 for anions: 350, $\bar{3}50$, 002	48 60	$a_c = b_c = 4.30$, $c_c = 1.99$, $\gamma_c = 123.81$ $a_a = b_a = 4.09$, $c_a = 1.93$, $\gamma_a = 136.33$	86, 89
Galenobismutite $PbBi_2S_4$ (space group *Pnma*, $Z = 4$, $N = 6/8$)				
$a = 11.742$, $b = 4.0814$, $c = 14.522$	for cations: 302, $\bar{3}02$, 020 for anions: $\bar{4}01$, 304, 020	24 38	$a_c = b_c = 4.12$, $c_c = 2.04$, $\gamma_c = 123.35$ $a_a = 3.30$, $b_a = 3.10$, $c_a = 2.04$, $\gamma_a = 126$	86, 89
Rouxelite $Cu_2HgPb_{22}Sb_{28}S_{64}(O,S)_2$ (space group *C*2/*m*, $Z = 2$, $N = 106/132$)				
$a = 43.113$, $b = 4.059$, $c = 37.874$, $\gamma = 117.35$	for cations: 1002, 0010, 020 for anions: $\bar{1}\bar{4}08$, 1002, 020	200 216	$a_c = 4.25$, $b_c = 4.31$, $c_c = 2.03$, $\gamma_c = 127.72$ $a_a = 4.46$, $b_a = 3.94$, $c_a = 2.03$, $\gamma_a = 130.14$	67, 86, 90
$Tm_{15}S_{22}$ (space group *C*2/*m*, $Z = 2$, $N = 30/44$)				
$a = 38.395$, $b = 3.842$, $c = 11.141$, $\beta = 91.0$	for cations: $\bar{1}\bar{0}02$, 003, 020 for anions: $\bar{1}\bar{0}02$, 204, 020	60 88	$a_c = 3.84$, $b_c = 4.47$, $c_c = 1.92$, $\gamma_c = 123.9$ $a_a = 3.54$, $b_a = 3.05$, $c_a = 1.92$, $\gamma_a = 115.68$	101
Cupromakopavonite $Cu_8Ag_3Pb_4Bi_{19}S_{38}$ (space group *C*2/*m*, $Z = \mathbf{1}$, $N = 34/38$)				
$a = 13.380$, $b = 4.0007$, $c = 31.083$, $\beta = 93.064$	for cations: 207, $20\bar{8}$, 020 for anions: 209, $20\bar{1}\bar{0}$, 020	60 76	$a_c = 4.03$, $b_c = 3.84$, $c_c = 2.00$, $\gamma_c = 63.52$ $a_a = 3.80$, $b_a = 3.64$, $c_a = 2.00$, $\gamma_a = 52.08$	102
Cuproneyite $Cu_7Pb_{27}Bi_{25}S_{68}$ (space group *C*2/*m*, $Z = 2$, $N = 118/136$)				
$a = 37.432$, $b = 4.0529$, $c = 43.545$, $\beta = 108.80$	for cations: 4010, $100\bar{3}$, 020 for anions: 4010, $80\bar{1}\bar{4}$, 020	224 272	$a_c = 3.69$, $b_c = 4.12$, $c_c = 2.03$, $\gamma_c = 114.85$ $a_a = 3.88$, $b_a = 3.39$, $c_a = 2.03$, $\gamma_a = 59.65$	103
Cosalite $Pb_2Bi_2S_5$ (*space group Pbnm*, $Z = 8$, $N = 32/40$)				
$a = 19.098$, $b = 23.890$, $c = 4.057$	for cations: $5\bar{3}0$, 530, 002	60	$a_c = b_c = 4.42$, $c_c = 2.03$, $\gamma_c = 128.79$	66, 91
Gladite $PbCuBi_5S_9$ (space group *Pnma*, $Z = 4$, $N = 28/36$)				
$a = 11.486$, $b = 4.003$, $c = 33.531$	for cations: 303, $10\bar{9}$, 020	60	$a_c = 3.62$, $b_c = 3.34$, $c_c = 2.001$, $\gamma_c = 89.06$	66, 92
Grumiplucite $HgBi_2S_4$ (space group *C*2/*m*, $Z = 4$, $N = 12/16$)				
$a = 14.164$, $b = 4.053$, $c = 13.967$, $\beta = 118.28$	for cations: $\bar{2}04$, 202, 020	24	$a_c = 4.03$, $b_c = 4.16$, $c_c = 2.03$, $\gamma_c = 119.78$	66, 93
Geocronite $Pb_{28}Sb_7As_5S_{46}$ (space group *P*2$_1$/*m*, $Z = 2$, $N = 80/92$)				
$a = 8.963$, $b = 31.93$, $c = 8.5$, $\beta = 118.02$	for cations: 100, 230, $\bar{2}42$	40	$a_c = 4.13$, $b_c = 4.25$, $c_c = 4.50$, $\alpha_c = 61.54$, $\beta_c = 121.50$, $\gamma_c = 124.53$	66, 94
Meneghinite $Pb_{13}CuSb_7S_{24}$ (space group *Pbnm*, $Z = 1$, $N = 21/24$)				
$a = 11.363$, $b = 24.057$, $c = 4.128$	for cations: 310, 170, 002	40	$a_c = 4.15$, $b_c = 3.65$, $c_c = 2.06$, $\gamma_c = 115.78$	66, 95
Eclarite $(Cu,Fe)Pb_9Bi_{12}S_{28}$ (space group *Pnma*, $Z = 4$, $N = 88/112$)				
$a = 54.76$, $b = 4.03$, $c = 22.75$	for cations: 1600, 1005, 020	160	$a_c = b_c = 4.45$, $c_c = 2.01$, $\gamma_c = 129.72$	66, 96
Paarite $Cu_{1.7}Pb_{1.7}Bi_{6.3}S_{12}$ (space group *Pmcn*, $Z = 5$, $N = 48.5/60$)				
$a = 4.007$, $b = 55.998$, $c = 11.512$	for cations: 0151, $0\bar{5}3$, 200	100	$a_c = 3.55$, $b_c = 3.63$, $c_c = 2.00$, $\gamma_c = 89.05$	66, 97
Pillaite $Pb_{9.167}Sb_{9.833}S_{23}$ $ClO_{0.5}$ (space group *C*2/*m*, $Z = 4$, $N = 76/98$)				
$a = 49.49$, $b = 4.13$, $c = 21.83$, $\beta = 99.62$	for cations: $\bar{1}\bar{0}05$, 206, 020	140	$a_c = 4.39$, $b_c = 4.31$, $c_c = 2.06$, $\gamma_c = 126.37$	66, 98
Zinkenite $Pb_{1.6}Sb_{3.4}S_7$ (space group *P*6$_3$, $Z = 6$, $N = 30/42$)				
$a = 22.12$, $c = 4.32$	for cations: 150, $5\bar{6}0$, 002	62	$a_c = b_c = 3.97$, $c_c = 2.16$, $\gamma_c = 120$	66, 99
Robinsonite $Pb_4Sb_6S_{13}$ (space group *P*1, $Z = 2$, $N = 20/26$)				
$a = 16.56$, $b = 17.69$, $c = 3.982$, $\alpha = 91.09$, $\beta = 96.46$, $\gamma = 96.77$	for cations: $\bar{4}30$, 050, $11\bar{2}$	40	$a_c = 4.11$, $b_c = 4.08$, $c_c = 1.99$, $\alpha_c = 85.07$, $\beta_c = 90.45$, $\gamma_c = 120.09$	66, 100
$BaBi_2S_4$ (space group *P*6$_3$/*m*, $Z = 9$, $N = 27/36$)				
$a = 21.705$, $c = 4.158$	for anions: 520, $\bar{7}50$, 020	78	$a_a = b_a = 3.50$, $c_a = 2.08$, $\alpha_a = \beta_a = 90$, $\gamma_a = 60$	69, 86

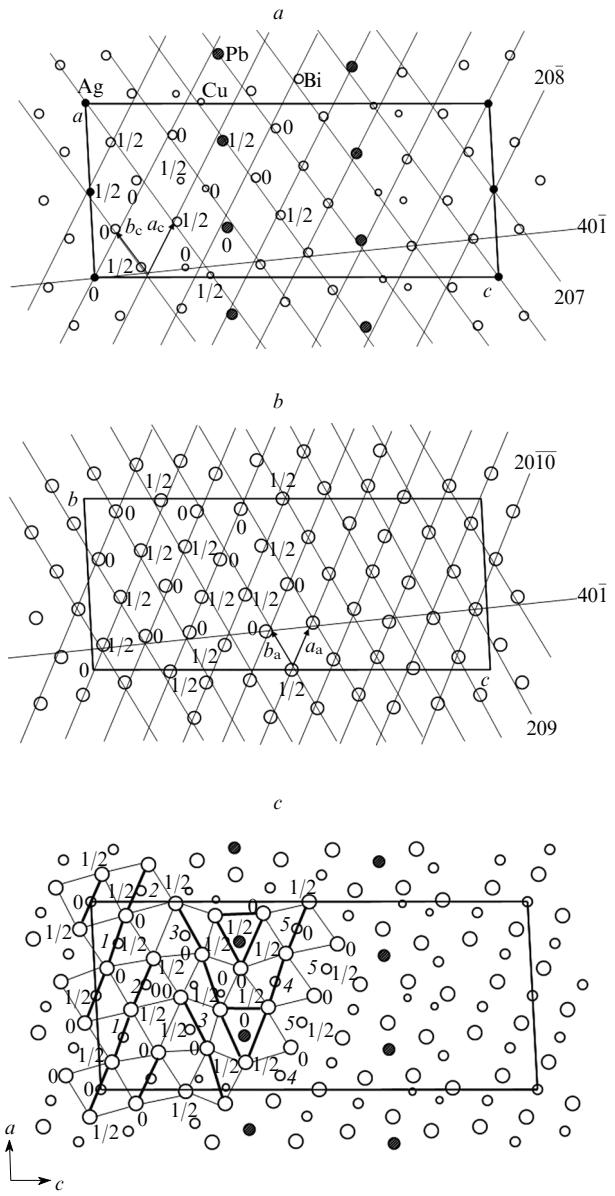


Figure 15. Structure of $Cu_8Ag_3Pb_4Bi_{19}S_{38}$.
(*a*) Cation positions projected onto the *xz* plane. In addition to the cross-sections of the projection by the (207) and (20$\bar{8}$) planes, the trace of the (40$\bar{1}$) plane is shown. In the left part of the unit cell, the coordinate *y* (0, 1/2) is given for the atoms; (*b*) the projection of the sulfur anion positions onto the *xz* plane; (*c*) the projection of cations and anions onto the *xz* plane. The Pb cations in the centres of the [6S] prisms, the Bi cations (designated with the numerals *1*–*5*) in the [6S] octahedra like Ag in the origin of coordinates; the edges of the polyhedra lying in the (020) planes are highlighted.

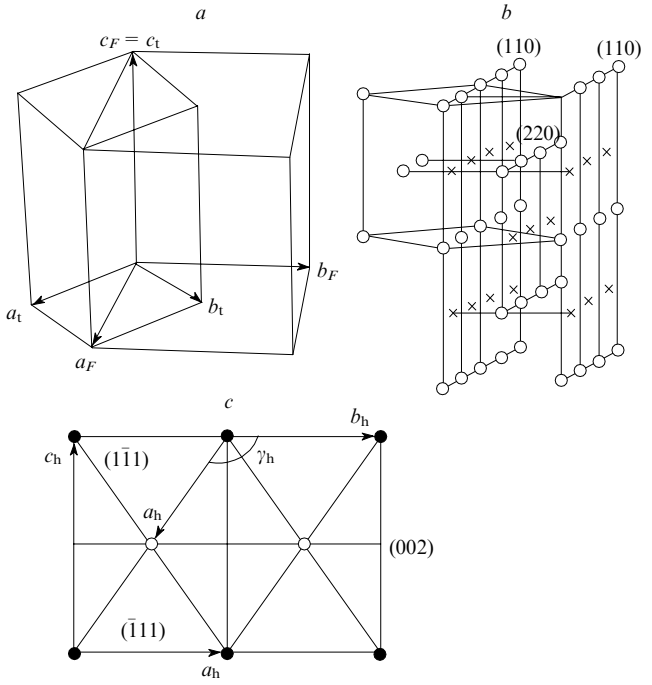


Figure 16. Selection of the a_t, b_t, c_t translations of the tetragonal I_t unit cell in the starting cubic *F* unit cell (*a*); (*b*) networks of lattice points that centre each other in the (020) planes of the I_t unit cell in the galenite-type structure.
Crosses mark vacant sublattice points with the following translations: a_t equal to one-half of the diagonal of the cube face lying in the (110) plane; c_t equal to the vertical edge of the cube; $b_t/2$ equal to 1/4 of the diagonal of the cube face perpendicular to the (110) plane; (*c*) is the sublattice with the pseudohexagonal subcell characteristic of lozenge-shaped structures formed by the {220} and {111} planes in the galenite-type structure. Atoms occupy one-half of the lattice points at two hights along the b_t direction (empty and filled circles).

structures if they are described, as described above, in the pseudohexagonal subcell (Fig. 16 *c*) containing one-half of vacant sites.

Therefore, monoclinic and orthorhombic lozenge-shaped structures can be considered as the first step in the formation of a cubic structure, in which the ordering of atomic positions is performed by one system of mirror planes. Due to the complex atomic composition, the ordering by means of mirror planes to form other orientations is impossible, and the process is terminated. It is convenient to use representations of cation and anion frameworks as two rectangular networks of lattice points that centre each other (a fragment of the galena structure) to find such fragments in lozenge-shaped structures.[104]

The results of crystallographic analysis of microtwinned structures (in particular, the structures of lillianite, β-lillianite and heyrovskyite, see Table 10) were quite unexpected.[63] It appeared that the mirror plane relates two parts of the structure within the unit cell, thus seemingly violating the ordering of atomic positions by a single system of (*hkl*) planes. Figure 17 *a* presents the projection of the cation positions along the short *c* axis of the lillianite structure. The cation positions are arranged according to the galena structure type by means of rectangular networks located at two heights and centring each other.[17, 80] The mirror planes perpendicular to the *b* axis adjoin the layers of this structure in different orientations (microtwinning). However, the crystallographic analysis showed that all cation positions in the structure are ordered by the crystallographic (250) and ($\bar{2}$50) planes and their derivative (400) with the (002) planes (see Table 10). The results of ordering can be seen in Fig. 17 *b*. This means that the mutual orientation of the fragments in the galena structure is not random but occurs within the common cation framework formed by the (250), ($\bar{2}$50) and (002) planes. Different orientations of the fragments can be obtained due to the presence of vacant sites in the cation framework.

Therefore, if the distribution of cations over two mirror planes at $z = 0$ and $z = 1/2$ is ignored, the common galena-

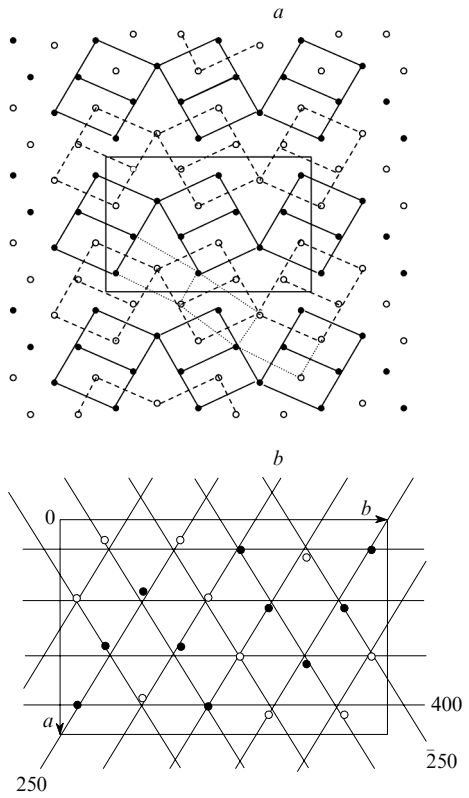


Figure 17. Structure of lillianite.[63]
(*a*) The representation of the cation matrix of lillianite by layers twinned by a mirror plane perpendicular to the *b* axis ($y = 1/4, 3/4$) in the PbS-type structure. Two adjacent $\{110\}_{PbS}$ planes are indicated by solid and dashed lines; the possible occurrence of the common PbS structure in the case of the rearrangement of cations along the *z* coordinate (with a loss of mirror microtwinning); (*b*) the *xy* projection of the cation positions and nodes of the sublattice formed by the intersection of families of the (250) and ($\bar{2}50$) crystallographic planes and of their derived (400) plane with the (002) planes. Hereinafter, the empty and filled points correspond to two heights along the *z* coordinate.

type structure can be constructed in the whole unit cell (in Fig. 17 *a*, the dashed lines indicate the possible propagation of the rectangular network through the microtwin mirror plane). If one-half of lattice points in the cation framework are vacant, the symmetry of the structure can be increased by relating its fragments by an additional mirror plane.

A similar situation takes place in the anion frameworks of the lillianite, β-lillianite and heyrovskyite structures.[63]

IV.3. Role of the Tl^+ cation in the structure formation of sulfides

In classical crystal chemistry relying on the principle of the close packing of anions as the bulkiest components of the crystal structure, large cations are considered as the exclusion and their active involvement in this process is assumed.[105,106] The well-known structure of perovskite $CaTiO_3$ is an example of the combined cation–anion packing that is formed by calcium and oxygen ions, whereas smaller Ti^{4+} cations occupy octahedral voids.[36] The Cs^+, Tl^+, Rb^+ and, probably, Ba^{2+} cations can be commensurate for the larger S^{2-} anion.

The crystallographic analysis was performed for a series of relatively simple structures[107] and for two minerals of rather complex composition — vrbaite and gabrielite.[108] The intensities of X-ray reflections were calculated only for cations, including Tl^+, only for anions and for anions together with Tl^+ cations. In these three cases, the most intense (skeletal) planes were examined for the real presence of pseudotranslational sublattices for cations, anions and anions together with thallium. The experimental data for these structures are summarized in Table 11.[109–119]

Among simple structures, there are structures with mirror planes perpendicular to the translation ~4 Å (see the previous section). The real atomic positions and networks of lattice points in the corresponding sublattices for the $TlIn_3S_5$ and $TlCr_2V_3S_8$ structures are shown in Figs 18 *a*,*b* and 19 *a*,*b*, respectively. The role of skeletal planes in the structure formation for both cations with Tl^+ and cation-independent planes of anions with Tl^+, as well as the real positions of Tl^+ cations in these structures, are of no doubt.

Let us consider gabrielite ($Tl_2AgCu_2As_3S_7$) as a structure of complex composition. The fact that the symmetry of this structure includes only a centre of symmetry attests to problems with ordering, primarily of the cations having diverse sizes and different crystal-chemical characteristics. The best results that were obtained by means of the 'most successful' (300), (005) and (331) planes are presented in the projection of cation positions along the *y* axis (Fig. 20 *a*) and in one of the cross-sections of the structure ($z = 0.1 \pm \Delta$, Fig. 20 *b*). The situation is much better for the ordering of anions and Tl^+ cations, although the parameters of the sublattice of anions and Tl^+ are related to the unit cell parameters in a very complex way (see Table 11). Thus, the subcell comprises 1/77 of the unit cell, the geometry of the subcell is similar to primitive cubic, and only 54 of a total of 77 lattice points are occupied. The quality of ordering can be seen in Fig. 20 *c*, which shows the real positions of sulfur and thallium atoms in one of the

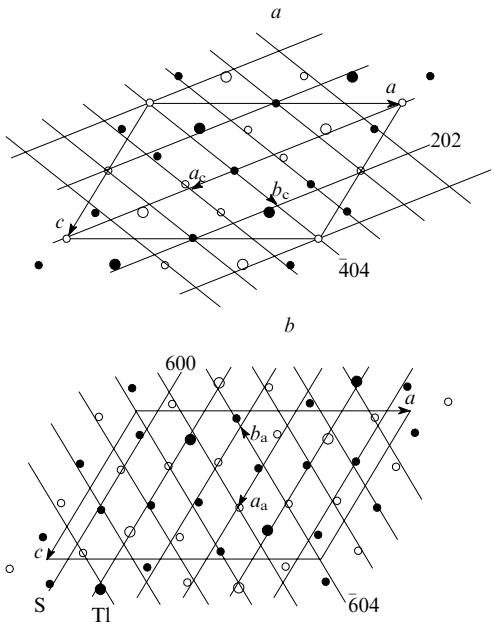


Figure 18. Structure of $TlIn_3S_5$.[107]
(*a*) The projection of cation positions onto the *xz* plane and the traces of skeletal cation planes (small circles represent In^{3+} cations) intersecting the *xz* plane; (*b*) the projection of anion positions with Tl^+ cations. Empty and filled circles correspond to positions at two heights.

Table 11. Results of crystallographic analysis of lozenge-shaped structures of sulfides with Tl^+.

Unit cell parameters	Anion sublattice with Tl					Cation sublattice					Ref.
	sublattice planes *hkl*	number of lattice points per unit cell	transformation matrix to the subcell	V_c/V_0	parameters of the anion subcell	sublattice planes *hkl*	number of lattice points per unit cell	transformation matrix to the subcell	V_c/V_0	parameters of the cation subcell	
Talcusite $TlCu_2S_2$ (space group $I\bar{4}/mmm$, $Z = 2$, $N = 6/6$)											
$a = 3.777$, $c = 13.3791$	$\bar{1}03$, 103, 020	12	$-1/2\ 0\ 1/6$ $1/2\ 0\ 1/6$ $0\ 1/2\ 0$	1/12	$a_a = b_a = 2.92$ $c_a = 1.89$ $\gamma_a = 80.52$	004, 200, 020	16	$1/2\ 0\ 0$ $0\ 0\ -1/4$ $0\ 1/2\ 0$	1/8	$a_c = c_c = 1.89$, $b_c = 3.34$	109
$TlCu_7S_4$ (space group $I4$, $Z = 2$, $N = 16/10$)											
$a = 10.174$, $c = 3.8389$	310, $\bar{1}30$, 002	20	$3/10\ 1/10\ 0$ $-1/10\ 3/10\ 0$ $0\ 0\ 1/2$	1/20	$a_a = b_a = 3.22$ $c_a = 1.92$	130, $\bar{3}10$, 002	20	$1/10\ 3/10\ 0$ $-3/10\ 1/10\ 0$ $0\ 0\ 1/2$	1/20	$a_c = b_c = 3.22$, $c_c = 1.92$	110
$TlTaS_3$ (space group $Pnma$, Z = 4, $N = 8/16$)											
$a = 9.228$, $b = 3.503$, $c = 14.209$	$\bar{2}04$, 204, 020	32	$-1/4\ 0\ 1/8$ $1/4\ 0\ 1/8$ $0\ 1/2\ 0$	1/32	$a_a = b_a = 2.91$ $c_a = 1.75$ $\gamma_a = 104.82$	103, 301, 020	16	$-1/8\ 0\ 3/8$ $3/8\ 0\ -1/8$ $0\ 1/2\ 0$	1/16	$a_c = 5.45$, $b_c = 3.89$, $c_c = 1.75$, $\gamma_c = 129.38$	111
$TlIn_3S_5$ (space group $C2/m$, $Z = 4$, $N = 16/24$)											
$a = 20.258$, $b = 3.8259$, $c = 12.821$, $\beta = 121.39$	$\bar{6}04$, 600, 020	48	$0\ 0\ 1/4$ $-1/6\ 0\ -1/4$ $0\ 1/2\ 0$	1/48	$a_a = 3.21$, $b_a = 3.22$ $c_a = 1.91$ $\gamma_a = 116.66$	$\bar{4}04$, 202, 020	32	$-1/8\ 0\ 1/8$ $1/4\ 0\ 1/4$ $0\ 1/2\ 0$	1/32	$a_c = 3.63$, $b_c = 4.36$, $c_c = 1.91$, $\gamma_c = 119.02$	112
$TlIn_5S_8$ (space group $C2/m$, $Z = 2$, $N = 12/18$)											
$a = 19.050$, $b = 3.839$, $c = 9.192$, $\beta = 102.94$	$\bar{6}02$, 003, 020	36	$-1/5\ 0\ 0$ $1/9\ 0\ 1/3$ $0\ 1/2\ 0$	1/36	$a_a = 3.18$, $b_a = 3.31$, $c_a = 1.92$, $\gamma_a = 115.6$	$\bar{6}01$, 202, 020	28	$1/7\ 0\ -1/7$ $1/14\ 0\ 3/7$ $0\ 1/2\ 0$	1/28	$a_c = 3.28$, $b_c = 3.87$, $c_c = 1.92$, $\gamma_c = 105.89$	113
$TlCr_2V_3S_8$ (space group $C2/m$, $Z = 2$, $N = 12/18$)											
$a = 17.643$, $b = 3.371$, $c = 8.54$, $\beta = 104.494$	$\bar{6}02$, 003, 020	36	$-1/6\ 0\ 0$ $1/9\ 0\ 1/3$ $0\ 1/2\ 0$	1/36	$a_a = 2.95$, $b_a = 3.03$, $c_a = 1.87$ $\gamma_a = 114.46$	202, 600, 020	24	$0\ 0\ 1/2$ $1/6\ 0\ -1/6$ $0\ 1/2\ 0$	1/24	$a_c = 4.27$, $b_c = 3.58$, $c_c = 1.87$, $\gamma_c = 127.09$	114

Table 11 (continued).

Unit cell parameters	Anion sublattice with Tl					Cation sublattice					Ref.
	sublattice planes *hkl*	number of lattice points per unit cell	transformation matrix to the subcell	V_c/V_0	parameters of the anion subcell	sublattice planes *hkl*	number of lattice points per unit cell	transformation matrix to the subcell	V_c/V_0	parameters of the cation subcell	
Vrbaite $Hg_3Tl_4As_8Sb_2S_{20}$ (space group $C2ca$, $Z = 4$, $N = 68/96$)											
$a = 13.399$, $b = 23.389$, $c = 11.287$	244, $\bar{2}44$, 008	128	1/4 1/8 0 −1/4 1/8 0 0 −1/8 1/8	1/128	$a_a = b_a = 4.06$, $c_a = 3.37$, $\alpha_a = \beta_a = 128.63$ $\gamma_a = 87.97$	340, $\bar{3}40$, 004	96	1/6 −1/8 0 1/6 1/8 0 0 0 1/4	1/96	$a_c = b_c = 3.48$, $c_c = 3.35$, $\gamma_c = 114.48$	115
Gabrielite $Tl_2AgCu_2As_3S_7$ (space group $P\bar{1}Z = 6$, $N = 48/54$)											
$a = 12.138$, $b = 12.196$, $c = 15.944$, $\alpha = 78.537$, $\beta = 84.715$, $\gamma = 60.470$	324, $\bar{1}\bar{3}3$, $\bar{2}14$	77	15/77 2/77 1/11 −4/77 20/77 −1/110 −18/77 13/77 1/11	1/77	$a_a = 3.06$, $b_a = 2.98$, $c_a = 3.01$, $\alpha_a = 78.74$, $\beta_a = 98.61$, $\gamma_a = 81.01$	300, 005, 331	45	1/3 −1/3 0 0 1/3 0 −1/15 0 1/5	1/45	$a_c = 4.08$, $b_c = 4.07$, $c_c = 3.13$, $\alpha_c = 93.28$, $\beta_c = 88.67$, $\gamma_c = 120.47$	116
Ellisite Tl_3AsS_3 (space group R3m, $Z = 1$, $N = 4/6$)											
$a = 5.9967$, $\alpha = 105.88$	$\bar{1}\bar{1}2$, 111, $\bar{1}2\bar{1}$	9	−1/3 0 1/3 1/3 1/3 1/3 −1/3 1/3 0	1/9	$a_a = c_a = 3.19$, $b_a = 2.33$, $\alpha_a = \gamma_a = 90$, $\beta_a = 60$	$\bar{1}11$, 111, $11\bar{1}$	4	−1/2 1/2 0 1/2 0 1/2 0 1/2 −1/2	1/4	$a_c = c_c = 4.79$, $b_c = 3.61$, $\alpha_c = \gamma_c = 131.5$, $\beta_c = 60$	117
Fangite Tl_3AsS_4 (space group Pnma, $Z = 4$, $N = 16/28$)											
$a = 8.894$, $b = 10.855$, $c = 9.079$	130, $\bar{2}30$, 013	36	1/4 1/6 −1/18 −1/4 1/6 −1/18 0 0 1/3	1/36	$a_a = b_a = 2.91$, $c_a = 3.03$, $\alpha_a = \beta_a = 99.98$, $\gamma_a = 99.63$	201, 03$\bar{1}$, 022	16	1/2 0 0 1/8 1/4 −1/4 −3/16 1/8 3/8	1/16	$a_c = 4.45$, $b_c = 3.71$, $c_c = 4.03$, $\alpha_c = 103.3$, $\beta_c = 114.5$, $\gamma_c = 72.6$	118
Lorandite $TlAsS_2$ (space group $P2_1/a$, $Z = 8$, $N = 16/24$)											
$a = 12.296$, $b = 11.313$, $c = 6.114$, $\beta = 104.21$	400, 140, 020	32	1/4 −1/16 0 0 1/4 0 0 0 1/2	1/32	$a_a = 3.15$, $b_a = 2.83$, $c_a = 3.06$, $\alpha_a = 90$, $\beta_a = 103.8$, $\gamma_a = 103$	1$\bar{4}$0, 340, 002	32	1/4 −3/16 0 1/4 1/16 0 0 0 1/2	1/32	$a_c = 3.73$, $b_c = 3.15$, $c_c = 3.06$, $\alpha_c = 103.8$, $\beta_c = 101.7$, $\gamma_c = 47.6$	119

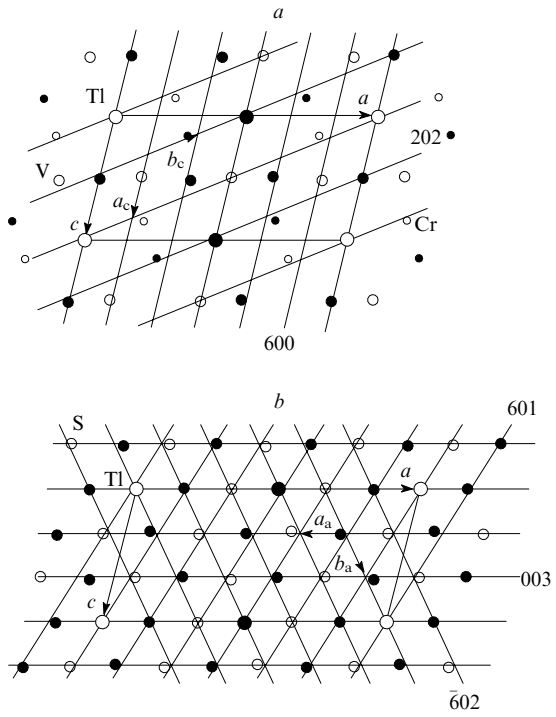


Figure 19. Structure of $TlCr_2V_3S_8$.[107]
(*a*) The projection of cation positions onto the *xz* plane and the traces of skeletal cation planes intersecting the former plane; (*b*) the projection of anion positions with Tl^+ cations. Empty and filled circles correspond to positions at two heights.

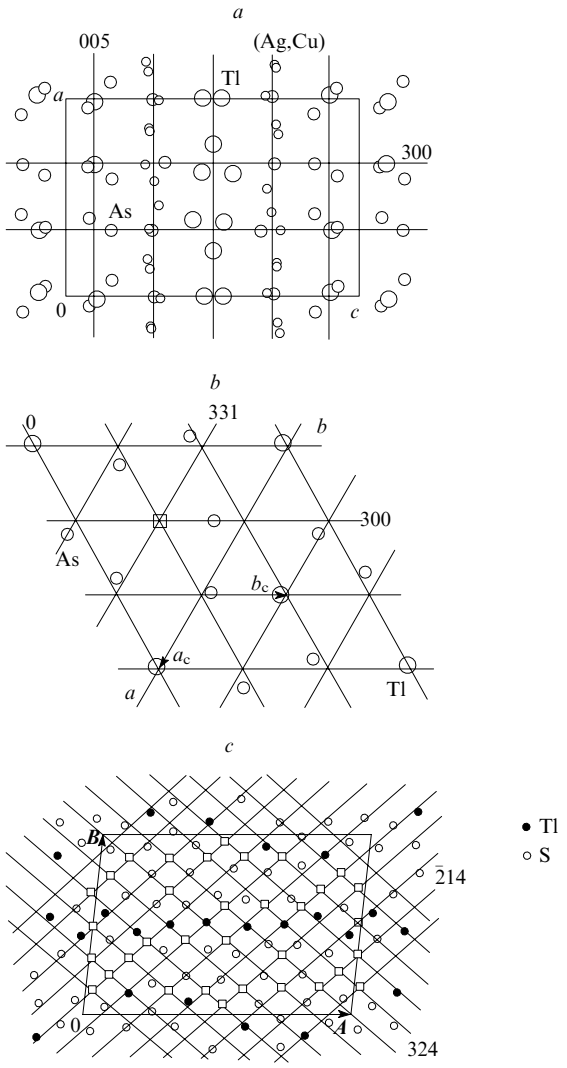


Figure 20. Structure of gabrielite $Tl_2AgCu_2As_3S_7$.[108]
(*a*) The projection of Tl, As, (Cu,Ag) cations along the *b* axis. The traces of the skeletal cation planes (300) and (005) are displayed; (*b*) the *xy* projection of thallium and arsenic cations in the layer at $z = 0.1 \pm \Delta$. The traces of the skeletal planes of the cation sublattice, (300) and (331), intersecting the (005) plane at $z = 0.1$ are shown. The translations a_c and b_c and the pronounced vacancy (□) are depicted; (*c*) the basis face of the expanded unit cell in the crystallographic plane $(\bar{1}\bar{3}3)$, its translations $\boldsymbol{A} = 3\boldsymbol{a} - \boldsymbol{b} = 32.20$ Å, $\boldsymbol{B} = \boldsymbol{b} + \boldsymbol{c} = 21.91$ Å, $\gamma = 83.1°$. A network of nodes as the points of intersection of the skeletal planes (324) and $(\bar{2}14)$ planes and the positions of thallium and arsenic atoms in the vicinity of these nodes (< 0.5 Å) are displayed. All 12 thallium atoms and 34 (of 42) sulfur atoms are present in the network; □ is a vacancy.

coordinate planes of the sublattice $(\bar{1}\bar{3}3)$ and a network of sublattice points. The structure as a whole is a superposition of two such parallel planes. It should be noted that the translations $\boldsymbol{A}$ and $\boldsymbol{B}$ are the translations of the so-called expanded unit cell[84] that is convenient for the adequate representation of the structure.

In addition to the structures listed in Table 11, the crystallographic analysis was performed for the Tl_2S structure (the mineral carlinite).[120, 121] This analysis resulted in the interesting interpretation of the structure in the galena structure type, although it was described in the '*anti*'-CdI_2 structure type but with considerable deformations of the latter. The structure of carlinite is, in fact, of an intermediate type and, consequently, it can be considered as an example of layered isomorphism, where the regular alternation of cationic and anionic layers (of the galena type) changes for the alternation of two cationic and one anionic layers. The compound $Tl_{18}Pb_2Ti_7S_{25}$ also have a very specific structure (see below).

For all structures, the inclusion of the large and (which is more important for the crystal formation) bulky Tl^+ cation in the anion sublattice is consistent with its geometry. In other words, thallium ions occupy vacant sites in the anion sublattice, *i.e.*, are involved in this sublattice along with S^{2-} anions. Presumably, the involvement of thallium substantially contributes to the regularity of this sublattice.

Let us note additional conditions for the congruence between two types of sublattices in these and other similar structures: apart from the above-mentioned requirement of the commensurability of the cation and anion sublattices, where the translational lattice should contain an integer number of both types of subcells, the sublattices have coinciding lattice points in all Tl^+ sites in the unit cell. At these sites, the sublattices are 'spot-welded', thus fixing their shifts with respect to each other, and this is obviously a more stringent requirement for the mutual arrangement of the atoms.

V. Crystallographic analysis of compounds with cluster fragments

The assumption that the forces responsible for the long-range order are much weaker than the forces that determine the coordination environment of the atoms was confirmed by the results of crystallographic analysis of compounds possessing small groups of atoms, in which the latter are

Table 12. Relative densities of filling with mercury atoms (ρ_{Hg}) and the centres of [Hg_2] dumbbell (ρ_c) of the most close-packed (*hkl*) planes in eglestonite.

hkl	d_{hkl}	ρ_{Hg}	*hkl*	d_{hkl}	ρ_c
004	4.01	0.51	004	4.01	0.90
224	3.27	0.48	044	2.83	0.95
026	2.54	0.45	444	2.31	0.94
444	2.31	0.35	008	2.00	0.92

linked by strong chemical bonds. The analysis was perfromed for a series of structures with dumbbell ($[Hg_2]^{2+}$) and triangular ($[Hg_3]^{4+}$) clusters, which can form common sublattices with both anions of similar volumes (iodide, bromide, chloride) and polyamions, such as $[SbO_6]^{7-}$, $[SbO_6]^{9-}$ and $[AsO_4]^{3-}$, the positions of which in the structures, like the positions of mercury clusters, are determined by the centres of mass of the groups.[122–132]

Generally, the search for close-packed crystallographic planes of cations in such structures did not give satisfactory results, but the situation becomes much better, if the geometric centres (that coincide with the centres of mass) of the groups of atoms are used instead of individual atoms involved in the clusters and the scattering atoms are placed in these centres. In other words, the crystallographic planes that are responsible for the structure formation cause virtually no internal structure distortions of the cluster groups and lead to the ordering of the centres of these groups (*i.e.*, bring them closer to the planes). The structure of cubic eglestonite $[Hg_2]_3Cl_3O_2H$ is a classical example.[131] For this mineral, the relative densities of mercury atoms and of the centres of [Hg_2] dumbbell pairs are given in Table 12. Figure 21 *a* presents the mercury sites in the (444) plane, and Fig. 21 *b* shows the positions of the centres of [Hg_2] dumbbell pairs. Therefore, the effects of ordering can be visually estimated. The data on the sublattices formed by the centres of the $[Hg_2]^{2+}$ and $[Hg_3]^{4+}$ clusters including the centres of other atomic groups or individual bulky atoms (Cl,Br) are summarized in Table 13. Figure 22 *a* presents, as an example, the arrangement of centres of [Hg_2] dumbbell

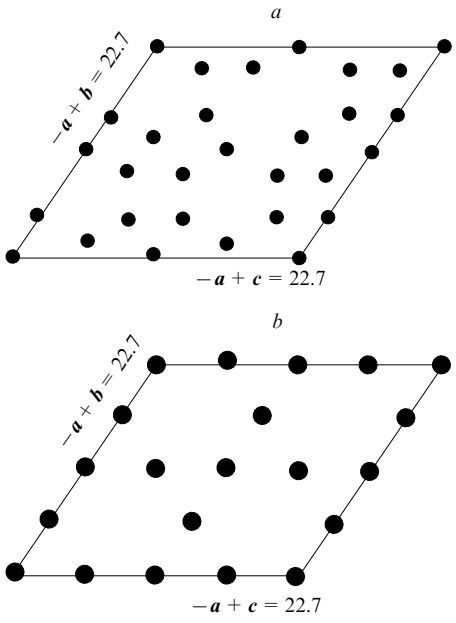


Figure 21. Cross-section of the eglestonite structure by the (444) plane.[16] (*a*) The arrangement of mercury atoms; (*b*) the arrangement of $[Hg_2]^{2+}$ dumbbells.

pairs and the centres of $[SbO_6]$ octahedra in the coordinate plane of the lattice for kelyanite $[Hg_2]_6SbO_6BrCl_2$ (Ref. 130) and a network of lattice points. The effect of ordering of these groups of atoms can be seen in their arrangement in one of the (003) planes of the structure, which is the (111) plane for the subcell (Fig. 22 *b*).

To sum up, the observed regularities in the structures of the compounds under consideration follow from the mechanical-wave concept of the crystalline state. In the improved form, the crystallographic analysis techniques can be used to study more complex anions, such as $[SiO_4]^{4-}$, $[PO_4]^{3-}$, $[SO_4]^{2-}$, *etc.*, which are ordered in the crystal structures as common building blocks, *i.e.*, which virtually retain their geometry.

Table 13. Crystallographic data for structures with cluster fragments.

Unit cell parameters	Skeletal planes for fragments	Number of lattice points per unit cell	Transformation matrix to the sublattice of fragments	V_c/V_0	Parameters of the cation subcell	Comments	Ref.
Poyarkovite $[Hg_2]_3Cl_2O_2$ (space group $C2/c$, $Z = 12$, number of cluster fragments in the unit cell: 36 [Hg_2])							
$a = 19.009$, $b = 9.01$, $c = 16.848$, $\beta = 110.82$	$\bar{2}04$, 600, 230	72	0 1/3 0 0 0 1/4 1/6 −1/6 1/12	1/72	$a_c = 3.01$, $b_c = 4.21$, $c_c = 3.33$, $\alpha_c = 85.35$, $\beta_c = 116.87$, $\gamma_c = 90$	centres of [Hg_2] occupy one-half of pseudohexagonal sublattice points	123, 133
Vasilyevite $[Hg_2]_{10}O_6I_3Br_2Cl(CO_3)$ [space group $\bar{P}$, $Z = 2$, number of cluster fragments in the unit cell: 20 [Hg_2], 6 I, 6 (Br,Cl), 2 (CO_3)]							
$a = 9.344$, $b = 10.653$, $c = 18.269$, $\alpha = 93.26$, $\beta = 90.55$, $\gamma = 115.42$	301, 032, 0$\bar{1}$4	42	1/3 0 0 −1/42 2/7 1/14 −1/14 −2/14 3/14	1/42	$a_c = 3.11$, $b_c = 3.34$, $c_c = 4.23$, $\alpha_c = 86.7$, $\beta_c = 90.7$, $\gamma_c = 117.5$	centres of [Hg_2], I, (Br,Cl) and (CO_3) are distributed over 42 pseudohexagonal sublattice points	134, 135

Table 13 (continued).

Unit cell parameters	Skeletal planes for fragments	Number of lattice points per unit cell	Transformation matrix to the sublattice of fragments	V_c/V_0	Parameters of the cation subcell	Comments	Ref.
Eglestonite $[Hg_2]_3Cl_3O_2$ (space group *Ia*3*d*, $Z = 16$, number of cluster fragments in the unit cell: 48 $[Hg_2]$, 48 Cl)							
$a = 16.036$	400, 040, 004	64	1/4 0 0 0 1/4 0 0 0 1/4	1/64	$a_c = b_c = c_c = 4.009$, $\alpha_c = \beta_c = \gamma_c = 90$	centres of $[Hg_2]$ and Cl form a *I*-cubic sublattice, 1/4 of lattice points are vacant	131
Shakhovite $[Hg_2]_2Sb(OH)_3O_3$ [space group *Im*, $Z = 2$, number of cluster fragments in the unit cell: 4 $[Hg_2]$, 2 (SbO_6H_3)]							
$a = 4.871$, $b = 15.098$, $c = 5.433$, $\beta = 98.86$	$\bar{1}01$, $1\bar{3}0$, 130	6	1/2 1/6 1/2 1/2 −1/6 1/2 0 0 1	1/6	$a_c = b_c = 4.20$, $c_c = 5.43$, $\alpha_c = \beta_c = 123.9$, $\gamma_c = 73.7$	centres of $[Hg_2]$ and (SbO_6H_3) occupy all sublattice points	136, 137
Kelyanite $[Hg_2]_6[SbO_6]BrCl_2$ (space group *P*3, $Z = 3$, number of cluster fragments in the unit cell: 18 $[Hg_2]$, 3 $[SbO_6]$)							
$a = b = 13.530$, $c = 10.004$, $\gamma = 120$	211, $\bar{3}21$, $1\bar{3}1$	21	5/21 4/21 1/3 −4/21 1/21 1/3 −1/21 −5/21 1/3	1/21	$a_c = b_c = c_c = 4.46$, $\alpha_c = \beta_c = \gamma_c = 70.17$	centres of $[Hg_2]$ and (SbO_6) octahedra occupy all sublattice points	130
Kuznetsovite $[Hg_3]AsO_4Cl$ (space group $P2_13$, $Z = 4$, number of cluster fragments in the unit cell: 4 $[Hg_2]$, 4 $[AsO_4]$)							
$a = 8.379$	200, 020, 002	8	1/2 0 0 0 1/2 0 0 0 1/2	1/8	$a_c = b_c = c_c = 4.19$, $\alpha_c = \beta_c = \gamma_c = 90$	centres of $[Hg_2]$ and (AsO_4) tetrahedra occupy all *P*-cubic sublattice points	122
α-Hg_2MoO_4 (α-$[Hg_2]MoO_4$) (space group *C*2/*c*, $Z = 4$, number of cluster fragments in the unit cell: 4 $[Hg_2]$, 4 Mo)							
$a = 8.735$, $b = 11.552$, $c = 4.931$, $\beta = 115.20$	200, 021, $0\bar{2}1$	8	1/2 0 0 0 1/4 1/2 0 −1/4 1/2	1/8	$a_c = 4.37$, $b_c = 3.88$, $c_c = 3.80$, $\alpha_c = 99.02$, $\beta_c = \gamma_c = 106.05$	centres of $[Hg_2]$ and Mo cations occupy all sublattice points	138
β-Hg_2MoO_4 (β-$[Hg_2]MoO_4$) (space group $P2_1/c$, $Z = 4$, number of cluster fragments in the unit cell: 4 $[Hg_2]$, 4 Mo)							
$a = 5.113$, $b = 9.018$, $c = 10.860$, $\beta = 101.01$	$\bar{1}02$, 102, 120	8	1 0 0 0 0 1/2 0 1/2 0	1/4	$a_c = 5.11$, $b_c = 5.43$, $c_c = 4.51$, $\alpha_c = \beta_c = 90$, $\gamma_c = 101.01$	centres of $[Hg_2]$ and Mo cations occupy all *I*-sublattice points	138
$Hg_2Mo_2O_7$ ($[Hg_2]Mo_2O_7$) (space group $P\bar{1}$, $Z = 2$, number of cluster fragments in the unit cell: 2 $[Hg_2]$, 4 Mo)							
$a = 7.097$, $b = 7.144$, $c = 8.038$, $\alpha = 64.89$, $\beta = 66.09$, $\gamma = 66.45$	112, $\bar{1}\bar{1}1$, 200	6	0 −2/3 1/3 1/2 −1/2 0 1/3 0 1/3	1/6	$a_c = 4.36$, $b_c = 3.90$, $c_c = 4.27$, $\alpha_c = 108.67$, $\beta_c = 111.62$ $\gamma_c = 53.80$	centres of $[Hg_2]$ and Mo cations occupy all sublattice points	139
$Hg_2Mo_5O_{16}$ ($[Hg_2]Mo_5O_{16}$) (space group *P*2/*c*, $Z = 2$, number of cluster fragments in the unit cell: 2 $[Hg_2]$, 10 Mo)							
$a = 9.139$, $b = 5.513$, $c = 14.289$, $\beta = 110.65$	013, $0\bar{1}3$, 202	12	−1/6 1/2 1/6 −1/6 −1/2 1/6 1/2 0 0	1/12	$a_c = b_c = 4.26$, $c_c = 4.57$, $\alpha_c = \beta_c = 123.69$, $\gamma_c = 80.64$	centres of $[Hg_2]$ and Mo cations occupy all sublattice points	140
$Hg_5Re_2O_{10}$ ($[Hg_2]_2HgRe_2O_{10}$) (space group $P2_1/b$, $Z = 2$, number of cluster fragments in the unit cell: 4 $[Hg_2]$, 2 Hg, 4 Re)							
$a = 6.401$, $b = 7.981$, $c = 11.538$, $\gamma = 98.87$	$\bar{1}20$, 013, 120	12	−1/2 1/4 −1/12 0 0 1/3 1/2 1/4 −1/12	1/12	$a_c = 4.14$, $b_c = 3.85$, $c_c = 3.63$, $\alpha_c = 105.36$, $\beta_c = 110.82$, $\gamma_c = 103.44$	centres of $[Hg_2]$ and the Re and Hg cations occupy 10 sublattice points; 2 sublattice points are vacant	141
Hg_2ReO_5 ($[Hg_2]_2Hg_2Re_2O_{10}$) (space group $P\bar{1}$, $Z = 4$, number of cluster fragments in the unit cell: 2 $[Hg_2]$, 4 Hg, 4 Re)							
$a = 7.95$, $b = 8.94$, $c = 9.01$, $\alpha = 114.11$ $\beta = 101.64$ $\gamma = 91.19$	$1\bar{2}1$, 111, $\bar{2}\bar{2}2$	12	−1/4 0 1/4 1/6 1/3 1/2 1/3 −1/3 0	1/12	$a_c = 3.29$, $b_c = 4.17$, $c_c = 4.03$, $\alpha_c = 98.13$, $\beta_c = 106.89$, $\gamma_c = 63.61$	centres of $[Hg_2]$ and the Re and Hg cations occupy 10 sublattice points, 2 sublattice points are vacant	142

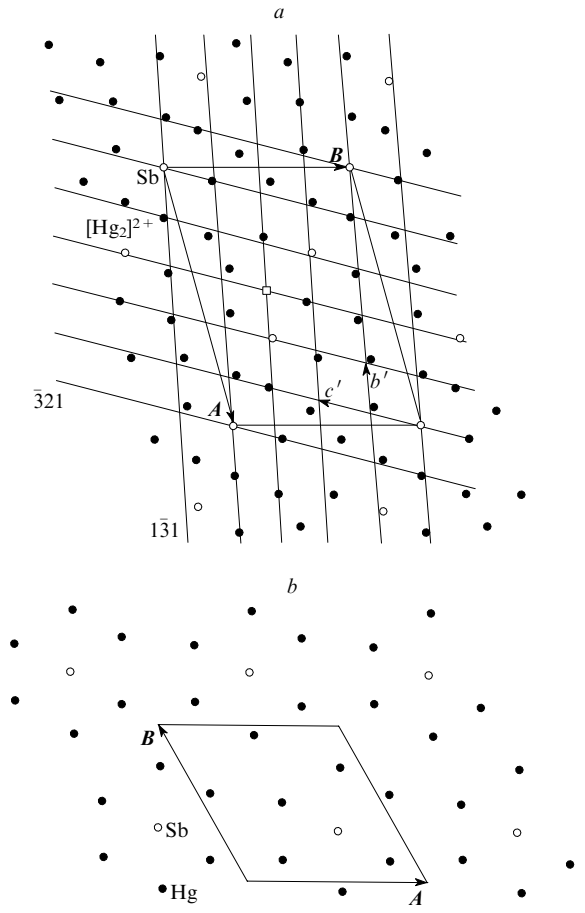


Figure 22. Structure of kelyanite $[Hg_2]_6SbO_6BrCl_2$.[16]
(*a*) The network of subllatice points formed by the intersection of the (211), ($\bar{3}21$) and ($1\bar{3}1$) planes in the (211) plane and the arrangement of the centres of $[Hg_2]^{2+}$ dumbbells and antimony atoms ($\boldsymbol{A} = \boldsymbol{a} - 2\boldsymbol{c} = 24.08$ and $\boldsymbol{B} = \boldsymbol{b} - \boldsymbol{c} = 16.80$ *AA*; $\gamma = 74.7°$, b' and c' are the sublattice parameters); (*b*) the arrangement of the centres of $[Hg_2]^{2+}$ dumbbells and antimony atoms on one of the (003) planes ($\boldsymbol{A} = \boldsymbol{a} = 13.53$ and $\boldsymbol{B} = \boldsymbol{b} = 113.53$ Å; $\gamma = 120°$).

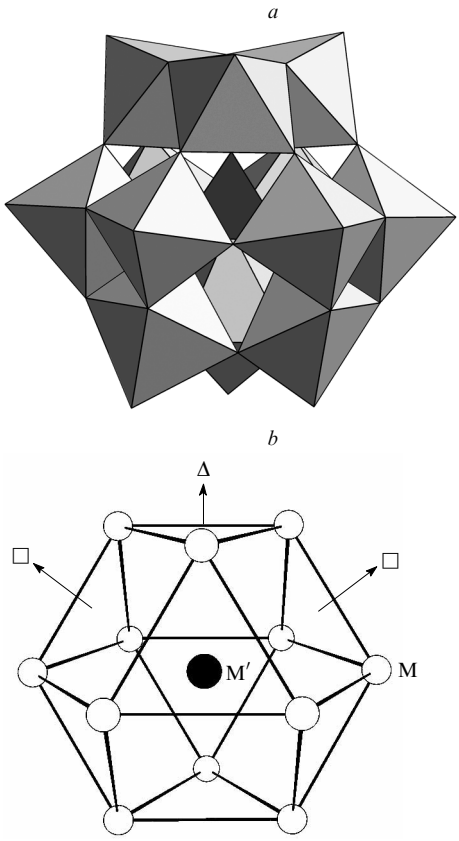


Figure 23. General view of the Keggin polyanion $[M'M_{12}O_{40}]$ (*a*) and its cation composition (*b*); (*a*) vertex- and edge-sharing WO_6 octahedra; *b*, the orientations of symmetry axes are depicted.

VI. Principle of coherent assembly of structures with large cluster blocks

The crystallographic analysis of compounds with Keggin-type polyanions, paratungstate ions, Dowson anions and their derivatives revealed a fundamental phenomenon in the organization of such structures referred to as coherent assembly.[143] In the study by Evans,[144] known structures with Keggin polyanions were classified according to the packing mode, and it was shown that polyanions always retain their structures in the resulting compounds. For the general formula $[M'M_{12}O_{40}]$ (M' = C, P, Si, Ge, V ...; M = W, Mo...), the Keggin polyanion comprises twelve edge- and vertex-sharing $[MO_6]$ octahedra with the inner $[M'O_4]$ tetrahedron (Fig. 23 *a*). The cations, taken separately, form a cuboctahedron containing a M' atom in the centre (Fig. 23 *b*). Based on the symmetry and geometry, this polyanion can be considered as a fragment of the close packing with trigonal atomic networks perpendicular to threefold axes arranged in the ABC order [11] and with square networks perpendicular to fourfold axes (Fig. 23 *b*). The crystallographic analysis of the close-packed planes of cations showed that in the crystal structures characterized by the combined packing of Keggin polyanions, fragments of trigonal and square networks of individual polyanions form common crystallographic planes passing throughout the crystal with a common network of lattice points.[143, 145] This fact is not trivial taking into account that up to 30 water molecules and up to ten cations and other fragments that neutralize the negative charge of the polyanion can exist per polyanion. These species create interlayers between adjacent polyanions and, consequently, the far-range ordering is required for the formation of common cation networks.

The effect of the common ordering of cation positions from individual and isolated building blocks was discovered in the structures with paratungstate ions $[H_2W_{12}O_{42}]^{10-}$ (Ref. 146) and in the structures with the Dowson polyanions $[H_2AsW_{18}O_{60}]^{7-}$. The general view of the latter and the cation positions on the (040) plane together with a network of lattice points formed by cross-sections of close-packed cation (424), ($\bar{4}06$) and ($\bar{8}22$) planes are shown in Fig. 24. The unit cell contains 160 (det $\{040/\bar{8}22/\bar{4}06\}$) lattice points of this cation subcell, 62 of which are occupied by tungsten atoms, since the polyanions are separated by water molecules and $(NH_4)^+$ cations in accord with the composition of the compound $(NH_4)_7[H_2AsW_{18}O_{60}]\cdot 16\,H_2O$.[147] The vacant lattice points of the cation network located between the adjacent polyanions are energetically favouable sites for any atoms and they are sometimes occupied by water oxygen atoms or light cations. The fact that heavy cations of the polyanions are packed to form a common network of the nodes of one sublattice is a direct consequence of their ordering by systems of crystallographic planes having different orientations.

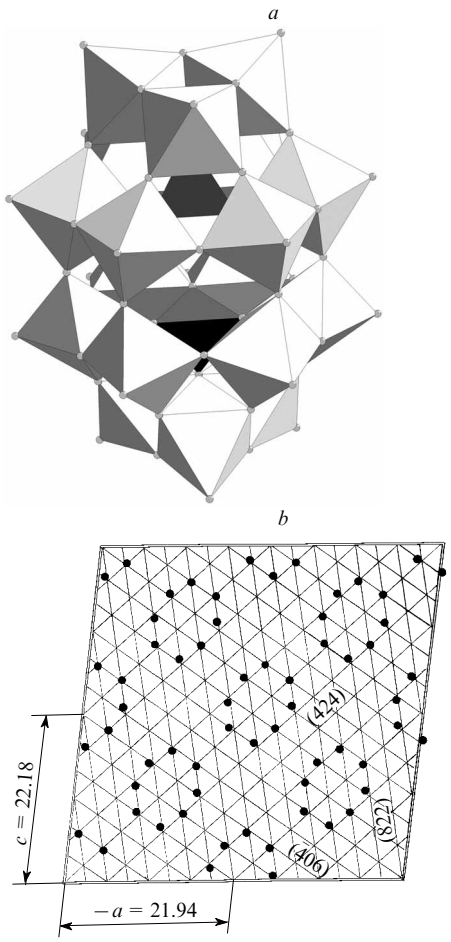


Figure 24. General view of the Dawson polyanion $[H_2AsW_{18}O_{60}]$ (*a*) and cation positions on the (040) plane with the network of lattice points formed by intersections of the close-packed planes (424), ($\bar{4}06$) and ($\bar{8}22$) (*b*).[16]

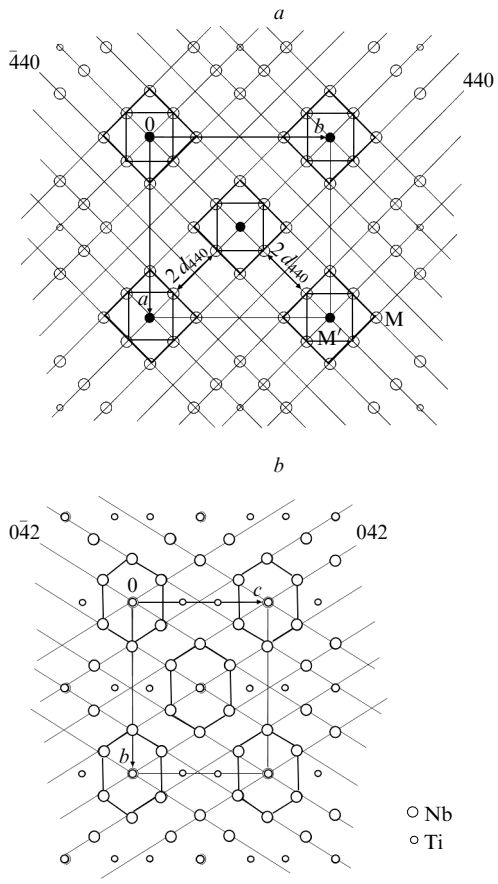


Figure 25. Structure of $Na_{12}[Ti_2O_2][SiNb_{12}]\cdot 4H_2O$: the projections of niobium and titanium cations onto the *xy* (*a*) and *yz* (*b*) planes.[143] The traces of cross-sections of the planes of the projections by perpendicular systems of crystallographic planes are shown; the projections of some polyanion positions are highlighted.

In the past years, studies on the chemistry of clusters and, in particular, on the structures of polyniobates [148] were actively developed, and the crystallographic analysis was performed for a number of these compounds.[143] Data on two structures of polyniobates are presented in Table 14.[149, 150] The high symmetry indicates that the ordering of atomic positions, primarily, of heavy cation positions reaches the maximum level. Actually, in the compound of the Keggin heteropolyanion with silicon, the cation sublattice of the cluster polanion is tetragonal, with the atomic positions coinciding well with the lattice points (Fig. 25 *a*).

The configuration of the Si and 12 Nb positions in $Na_{12}[Ti_2O_2][SiNb_{12}O_{40}]\cdot 4H_2O$ is similar to that shown in Fig. 23 *b*. The fourfold axis is perpendicular to the *ab* plane so that the network of the cation sublattice is square. The effect of coherent assembly results in that the cation positions in the structure determine the packing of its fragments virtually regardless of the positions of the other atoms. The polyanions take the same orientation due to the presence of translational symmetry, and the distances between adjacent skeletal cation cores, which are $2d_{440}$ in the *xy* projection and d_{042} in the *yz* projection (Fig. 25), are the consequence of the dominant ordering of heavy cations in the crystal structure formation.

In $Ba_2MgZr_4[BaNb_{12}O_{42}]\cdot 12H_2O$, the configuration of the cation positions of the $[BaNb_{12}O_{42}]^{22-}$ polyanion substantially differs from that described above, but the packing in the structure is also determined by their skeletal cores (Fig. 26). Since the structure is cubic, the distances between the polyanions in all three identical projections are specified by interplanar distances between

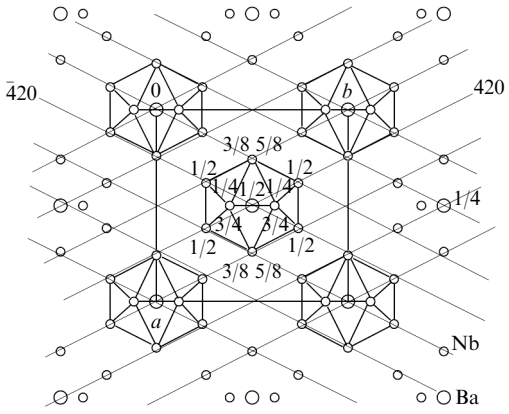


Figure 26. Structure of $Ba_2MgZr_4[BaNb_{12}O_{42}]\cdot 12H_2O$.
The projection of barium and niobium cations in the $BaNb_{12}O_{42}$ clusters and the traces of the cross-sections of the structure by the (420) and ($\bar{4}20$) planes. The atomic coordinates *z* are given for the central cluster of the *I*-unit cell.

Table 14. Results of crystallographic analysis of the structures with large cluster blocks.

Unit cell parameters	Skeletal planes for the cation sublattice	Number of lattice points per unit cell	Transformation matrix to the cation sublattice	V_c/V_0	Cation sublattice parameters	Comments	Ref.
$(NH_4)[H_2AsW_{18}O_{60}]\cdot 16\,H_2O$ (space group $C2/c$, $Z = 4$, number of cations per unit cell: 72 W)							
$a = 21.937$, $b = 14.239$, $c = 22.177$, $\beta = 96.95$	040, $\bar{8}22$, $\bar{4}06$	160	3/40 1/4 1/20 −3/20 0 −1/10 1/20 0 2/10	1/160	$a_c = 4.02$, $b_c = 3.74$, $c_c = 4.44$, $\alpha_c = 133.32$, $\beta_c = 71.40$, $\gamma_c = 106.05$	of 160 sublattice points, 62 points are occupied by tungsten atoms	127, 147
$Na_{12}[Ti_2O_2][SiNb_{12}O_{40}]\cdot 4\,H_2O$ (space group $I\bar{4}m2$, $Z = 2$, number of cations per unit cell: 2 Si, 24 Nb)							
$a = 14.27$, $b = 14.27$, $c = 11.29$	440, $\bar{4}40$, 004	128	1/4 1/4 0 −1/4 1/4 0 0 0 1/20	1/16	$a_c = b_c = 5.04$, $c_c = 5.64$, $\alpha_c = \beta_c = \gamma_c = 90$	(Si, Nb) cations occupy a part of the points in the F-tetragonal sublattice with the doubled parameters a_c, b_c, c_c	143, 149
Menezesite $Ba_2MgZr_4[BaNb_{12}O_{42}]\cdot 12\,H_2O$ (space group $Im\bar{3}$, $Z = 2$, number of cations per unit cell: 2 Ba, 24 Nb)							
$a = 13.017$, $b = 13.017$, $c = 13.017$	024, 402, 240	72	−1/9 1/18 2/9 2/9 −1/9 1/18 1/18 2/9 −1/9	1/72	$a_c = b_c = c_c = 3.31$, $\alpha_c = \beta_c = \gamma_c = 106.6$	cations (Ba, Nb) of the cluster occupy a part of rhombohedral sublattice points	144, 150
$KNa_{23}O_4[\{Rh_4O_2(H_2O)\}(H_2W_9O_{33})_2]\cdot 48\,H_2O$ (space group $P\bar{1}$, $Z = 1$, number of cations per unit cell: 4 Rh, 18 W)							
$a = 12.441$, $b = 13.799$, $c = 14.621$, $\alpha = 98.835$, $\beta = 104.179$, $\gamma = 103.04$	213, $\bar{1}\bar{1}5$, $2\bar{4}4$	64	1/4 7/32 3/32 −1/4 1/32 5/32 1/8 −13/64 −1/64	1/64	$a_c = 3.62$, $b_c = 4.34$, $c_c = 3.50$, $\alpha_c = 125.03$, $\beta_c = 102.23$, $\gamma_c = 109.61$	cations (Rh, W) of the cluster occupy a part of sublattice points	152
$Tl_{18}Pb_2Ti_7S_{25}$ (space group $Pa3$, $Z = 4$, number of cations per unit cell: 72 Tl, 8 Pb, 28 Ti)							
$a = 17.095$, $b = 17.095$, $c = 17.095$	600, 060, 006	216	1/6 0 0 0 1/6 0 0 0 1/6	1/216	$a_c = b_c = c_c = 2.87$, $\alpha_c = \beta_c = \gamma_c = 90$	108 cations (Tl, Pb, Ti) occupy one-half of cation cubic sublattice points according to the *F*-lattice law with the doubled unit cell parameter	153, 154

the close-packed cation {420} planes and their symmetry-related analogues. The highly symmetric configuration of this polyanion is retained also in the case of an essentially different cation composition, namely, in the mineral aspedamite $(Fe^{3+},Fe^{2+})_3Nb_4[Th(Nb,Fe^{3+})_{12}O_{42}]\cdot(H_2O,OH)_{12}$ (Refs 143, 151).

The structure with the new polyoxyanion $[\{Rh_4O_2(H_2O)_2\}[H_2W_9O_{33})_2]$[152] is an example of coherent assembly from more complex fragments; the molecular symmetry of this polyanion includes only a centre of inversion (Table 14, Fig. 27). The cation skeleton of the polyanion can be described as a cuboctahedron cut into two parts across the hexagonal cross-section (see Fig. 23 *b*) accompanied by the transformation of the halves of W into the whole atoms and their separation by a quartet of rhodium cations that form a rhombus and lie in the plane parallel to the cross-section. All cations of the polyanion are in the close-packed cation (213) planes. Their arrangement in the unit cell is shown in Fig. 28 *a*, and the correspondence between the tungsten and rhodium cation positions and the sublattice points can be seen in the (213) plane taken as the basis of the expanded unit cell (Fig. 28 *b*).[84] The dominant effect of the common sublattice of positions of heavy tungsten and rhodium cations on the composition of the structure, including the total number of water molecules and sodium cations, is of no doubt.

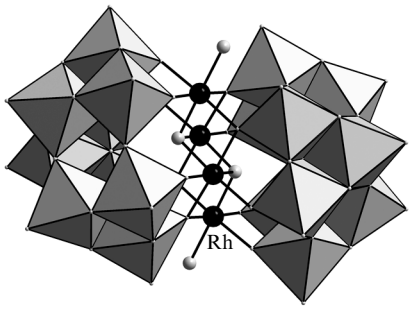


Figure 27. Structure of the polyoxyanion $[\{Rh_4O_2(H_2O)_2\}(H_2W_9O_{33})_2]$.[152]

The cubic structure of $Tl_{18}Pb_2Ti_7S_{25}$ [153, 154] (Table 14) is a unique example of the fulfillment of the following key conditions of the crystallization from the fragments that have been already formed in the precrystallization phase:

— the complementary of the packing due to the tendency to the minimum volume;

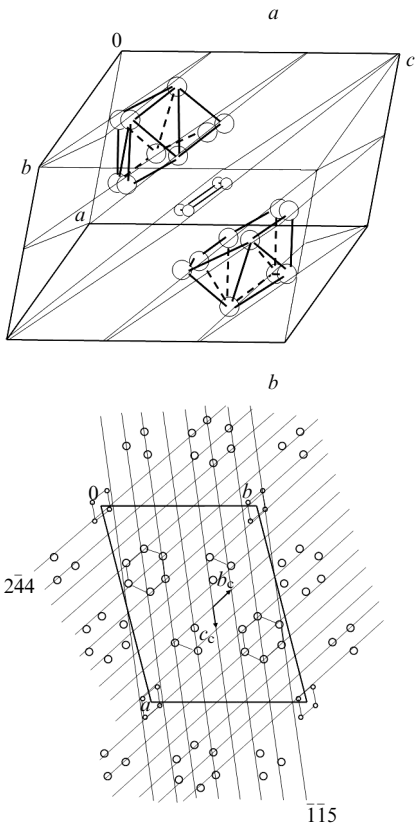


Figure 28. Structure of $KNa_{23}O_4(H_2O)_{48}[\{Rh_4O_2(H_2O)_2\}(H_2W_9O_{33})_2]$. (*a*) The arrangement of tungsten and rhodium cations in the cross-sections of the unit cell by the (213) planes; (*b*) the projections of tungsten and rhodium cations onto the (213) plane and the cross-sections of this projection by the other two coordinate planes of the cation sublattice: $(\bar{1}\bar{1}5)$ and $(2\bar{4}4)$.

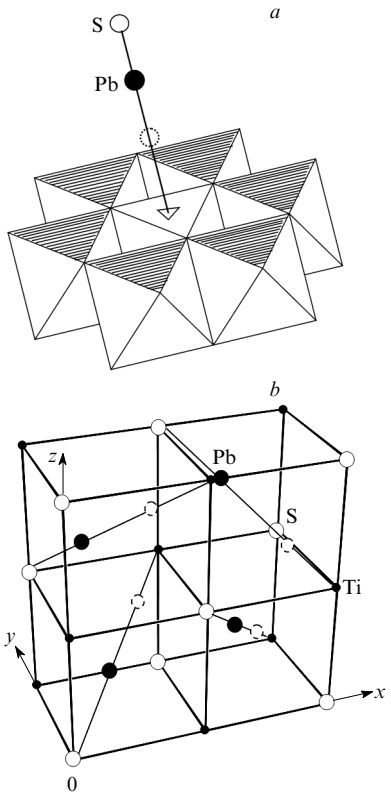


Figure 29. Supposed template of the $Tl_{18}Pb_2Ti_7S_{25}$ structure.[154] (*a*) A planar group formed by seven edge-sharing (TiS_6) octahedra with the perpendicular $\bar{3}$ axis passing through the central Ti atom. A vacant sulfur site (shaded circle), a lead cation and a sulfur atom in a special position with symmetry $\bar{3}$ are located on the $\bar{3}$ axis at equal distances from each other; (*b*) the mutual orientation of four non-intersecting $\bar{3}$ axes in one-half of the unit cell ($0 \leqslant x \leqslant 1$; $0 \leqslant y \leqslant 1/2$; $0 \leqslant z \leqslant 1$) of the structure. The positions of the central titanium atom, a vacant sulfur site (shaded circle), a lead cation and a sulfur atom are depicted to represent the combined packing of the structural fragments on the $\bar{3}$ axis.

— the coherence in the arrangement of atoms responsible for the structure formation;

— the maximum symmetry, which reduces the number of degrees of freedom of the objects that form the structure.

In the $Tl_{18}Pb_2Ti_7S_{25}$ structure, the $[Ti_7S_{24}]$ fragment has the strongest chemical bonds. The central $[TiS_6]$ octahedron is surrounded by six octahedra linked by sharing edges to form a planar group with the symmetry $\bar{3}$ (Fig. 29 *a*). The $\bar{3}$ axis passing through the central titanium atom perpendicular to the plane of the octahedra serves as a site for scanty lead cations and the basis sulfur atom that is not linked to the titanium atom. The crystallization of four such fragments with threefold axes in different directions are arranged to form a unit cell with the space group $Pa3$, in which these axes do not intersect each other (Fig. 29 *b*).

All cations of the structure form common trigonal planar networks of lattice points perpendicular to threefold axes. The fragments of these networks are sets of seven $[Ti_7S_{24}]$ groups. The same planar networks, but shifted with respect to the cation networks, are formed by all anions of the structure. Therefore, the structure is interpreted as the PbS (NaCl) structure type with the unit cell parameter three times as large as the initial one. The unit cell should contain $3^3 = 27$ subcells of the PbS type, *i.e.*, $27 \times 4 = 108$ cations. This corresponds to the real situation. However, there are only 100 anions, the vacant sulfur site being in a special position on the $\bar{3}$ axis between the Ti and Pb ions (Fig. 29 *a*).

For this structure, the sublattice with the parameter equal to one-half of the parameter of the *F*-lattice of the galena structure type is given in Table 14. In the ideal case, one-half of the lattice points are occupied by cations, and another half of these points are occupied by anions; besides, there are 8 vacancies. The effect of symmetrization of atomic positions resulted in that the structure containing 208 atoms per unit cell is characterized by only twelve coordinate parameters for cations and twelve parameters for anions.

In the past years, the term 'self-assembly' in solution applied to compounds with polyanions has appeared in the literature.[148, 152] The distinguishing feature of the synthesis of crystalline phases of these compounds is the energy gain due to the formation of large fragments with high local symmetry, both chemical interactions and the three-dimensional ordering being involved in this process. Therefore, such processes are characterized as the first crystallization step. The final step is the coherent assembly of these fragments, the other atoms playing a passive role.

The principle of coherent assembly took place in the above-considered microtwinning in the lillianite structure, because the stacking of layers in different orientations resulted in the distribution of atoms over the points of the lattice common for the whole structure.

VII. Conclusion

The fundamental differences in the structures of amorphous and crystalline phases of substances are that the latter possess the long-range order — the translational lattice, the formation of which is, as a rule, accompanied by a change in the molar volume and considerable energy evolution (the heat of crystallization). The crystallographic analysis relying on the mechanism of ordering of atomic positions by families of parallel equidistant planes can be used to study details of the ordering and their probable sequence. Almost in all cases, the application of this technique to structures of different classes of inorganic compounds revealed the pseudotranslational ordering of individual groups of atoms with the sublattice parameters of an order of interatomic contacts. The universal character of this phenomenon is a consequence of the mechanism of ordering due to the action of mechanical elastic forces.

The unified geometry of cation sublattices (common 'genome') established in the structures of sulfides can account for, in particular, the formation of widespread supergene mineral associations, which have different compositions and symmetry and in which epitaxial contacts and even intergrowth of structures occur due to this common sublattice.

The phenomenon of coherent assembly of structures from nanosized structured blocks considered in the previous section, on the one hand, provides additional convincing evidence for the mechanical-wave concept of the crystalline state and, on the other hand, determines the conditions of the design of new compounds from specified building blocks.

As mentioned above, the close-packed atomic planes employed in the crystallographic analysis contain the strongest interatomic bonds. In some cases, the structures of these planes remain virtually unchanged upon solid-phase transformations, by changing the mutual arrangement due to relative shifts.[16] In such investigations, the crystallographic analysis techniques will be very useful.

For the practical application of crystalline materials, their structures should be stable. From the available data it is clear that the stability of crystal structures depends not only on the strength of interatomic bonds but also on the symmetry, as well as on the relative mass of the regularly arranged key atoms. A high stability of symmetric cation skeletons can be seen for the structures of sulfides. Symmetry elements relate differently oriented families of skeletal planes, thus increasing the level of stability of the structures to variations in the composition and external conditions.

The problem of stability of structural frameworks comprising rigid groups connected by linear chains (linkers) is the order of day in view of the need in the targeted design of porous structures (gas containers, molecular sieves, separation of enantiomers and so on) that has risen in the past year.[155, 156] In order to design a framework with the desired geometry, it is necessary not only to choose the atomic composition but also to provide the arrangement of atoms such that a system of skeletal planes ensuring the ordering of atoms is highly symmetric and the network of their lattice points coincides with the positions of key (bulky) atoms or the positions of the centres of rigid groups of atoms, which are ordered as a single whole.

Based on the results obtained by crystallographic analysis, the following general sequence of crystallization steps can be proposed. In the precrystallization phase, in which the short-range order in the environment of atoms already occurs, the centres of rigid atomic fragments and the bulkiest atoms of the structure are ordered. This gives rise to a pseudotranslational lattice with the parameters similar to the contacts between the objects that are ordered (the skeleton of the structure). The further ordering concerns lighter fragments and individual atoms, but it only slightly changes the geometry of the skeleton and has to conform in order to form a common translational lattice. This scheme is not original. For example; it has been proposed in the studies by Anderson,[157, 158] but here it appears independently.

Therefore, the crystallographic analysis adds very valuable objective data to our understanding of the universal process of the transition of the matter to the most stable (crystalline) state.

This review has been written, in part, with the financial support of the Russian Scientific Foundation (Grant No. 13-05-00030).

References

1. J-G Eon *Struct. Chem.* **23** 987 (2012)
2. W E Klee *Cryst. Res. Technol.* **39** 959 (2004)
3. M O'Keeffe, B G Hyde *Phylos. Trans. R. Soc. London, Mathem. Phys. Sci.* **295** 553 (1980)
4. O Delgado-Friedrichs, M O'Keeffe *Acta Crystallogr. Sect. A* **59** 351 (2003)
5. J-G Eon *Acta Crystallogr. Sect. A* **67** 68 (2011)
6. O M Yaghi, M O'Keeffe, N W Ockwig, H K Chae, M Eddadoudi, J Kim *Nature (London)* **423** 705 (2003)
7. N W Ockwig, O Delgado-Friedrichs, M O'Keeffe *Acc. Chem. Res.* **38** 176 (2005)
8. O M Yaghi, M O'Keeffe, M Kanatzidis *J. Solid State Chem.* **152** 1 (2000)
9. M O'Keeffe, M A Peskov, S J Ramsden, O M Yaghi *Acc. Chem. Res.* **41** 1782 (2008)
10. O Delgado-Friedrichs, M D Foster, M O'Keeffe, D M Prospero, M M J Treasy, O M Yaghi *J. Solid State Chem.* **178** 2533 (2005)
11. W B Pearson *The Crystal Chemistry and Physics of Metals and Alloys* (New York: Wiley-Interscience, 1972)
12. *FIZ/NIST, Inorganic Crystal Data Base* (Gaitersburg: Karlsrue National Institute of Standard and Technology, 2010)
13. P I Kripyakevich *Strukturnye Tipy Intermetallicheskikh Soedinenii* (Structure Types of Intermetallic Compounds) (Moscow: Nauka, 1977)
14. N L Smirnova, L I Poteshnova *Vestn. Mosk. Univ.* (6) 13 (1966)
15. N A Bliznyuk, S V Borisov *J. Struct. Chem.* **33** 284 (1992) [*Zh. Strukt. Khim.* **33** (2) 145 (1992)]
16. S V Borisov, S A Magarill, N V Pervukhina *Algoritmy i Praktika Kristallograficheskogo Analiza Atomnykh Struktur* (Algorithms and Practice of Crystallographic Analysis of Atom Structures) (Novosibirsk: Siberian Branch of the Russian Academy of Sciences, 2012)
17. L Elcoro, J M Perez-Mato, K Friese, V Petříček, T Balić-Zunić, L A Olsen *Acta Crystallogr. Sect. A* **64** 684 (2008)
18. A L Loeb *Acta Crystallogr.* **15** 219 (1962)
19. S V Borisov *Crystallogr. Rep.* **45** 709 (2000) [*Kristallografiya* **45** 779 (2000)]
20. N A Bliznyuk, S V Borisov, E S Kuklina *J. Struct. Chem.* **35** 64 (1994) [*Zh. Strukt. Khim.* **35** (1) 71 (1994)]
21. S A Gromilov, E A Bykova, S V Borisov *Crystallogr. Rep.* **56** 947 (2011) [*Kristallografiya* **56** 1013 (2011)]
22. S V Borisov, N A Bliznyuk, E S Kuklina *J. Struct. Chem.* **35** 279 (1994) [*Zh. Strukt. Khim.* **35** (3) 3 (1994)]

23. N A Bliznyuk, S V Borisov, E S Kuklina, N V Podberezskaya *J. Struct. Chem.* **34** 764 (1993) [*Zh. Strukt. Khim.* **34** (5) 126 (1993)]
24. S V Borisov *J. Struct. Chem.* **37** 773 (1996) [*Zh. Strukt. Khim.* **37** (5) 907 (1996)]
25. S V Borisov, E N Ipatova *J. Struct. Chem.* **35** 865 (1994) [*Zh. Strukt. Khim.* **35** (6) 129 (1994)]
26. S V Borisov, E N Ipatova, E S Kuklina *J. Struct. Chem.* **36** 112 (1995) [*Zh. Strukt. Khim.* **36** (1) 128 (1995)]
27. S V Borisov, E N Ipatova, E S Kuklina *J. Struct. Chem.* **37** 278 (1996) [*Zh. Strukt. Khim.* **37** 319 (1996)]
28. S V Borisov *J. Struct. Chem.* **33** 871 (1992) [*Zh. Strukt. Khim.* **33** (6) 123 (1992)]
29. N N Mozgova, A I Tsepin *Bleklye Rudy* (Faded Ores) (Moscow: Nauka, 1983)
30. E A Pobedimskaya, L N Kaplunnik, I V Petrova, in *Kristallokhimiya (Itogi Nauki i Tekhniki)* [*Crystal Chemistry (Advances in Sciences and Engineering)*] Vol. 25 (Moscow: Izd. VINITI, 1991) p. 119
31. Y Moëlo, E Makovicky, N Mozgova, J L Jambor, N Cook, A Pring, W Paar, E H Nickel, S Graeser, S Karup-Møller, T Balić-Zunić, W G Mumme, F Vurro, D Topa *Eur. J. Mineral.* **20** 7 (2008)
32. E Makovicky *Eur. J. Mineral.* **5** 545 (1993)
33. E Makovicky, D Topa *Can. Mineral.* **47** 3 (2009)
34. S V Borisov, S A Magarill, N V Podberezskaya, N V Pervukhina *J. Struct. Chem.* **38** 759 (1997) [*Zh. Strukt. Khim.* **38** 908 (1997)]
35. S V Borisov, S A Magarill, N V Pervukhina *Fundam. Probl. Sovremen. Materialoved.* **7** (2) 104 (2010)
36. A F Wells *Structural Inorganic Chemistry* (Oxford: Clarendon Press, 1984)
37. S V Borisov, S A Magarill, N V Pervukhina *J. Struct. Chem.* **50** 853 (2009) [*Zh. Strukt. Khim.* **50** 890 (2009)]
38. S V Borisov, S A Magarill, N V Pervukhina *Crystallogr. Rep.* **54** 758 (2009) [*Kristallografiya* **54** 805 (2009)]
39. S V Borisov , S A Magarill, N V Pervukhina *J. Struct. Chem.* **50** (Suppl.) S104 (2009) [*Zh. Strukt. Khim.* **50** (Prilozhenie) S111 (2009)]
40. S V Borisov, S A Magarill, N V Pervukhina *Vestn. Hizhegorod. Gos. Univ., Ser. Fiz. Tv. Tela* (5) 55 (2009)
41. S A Magarill, S V Borisov, N V Pervukhina *Fundam. Probl. Sovremen. Materialoved.* **6** (4) 17 (2009)
42. S V Borisov, S A Magarill, N V Pervukhina *Zap. Ros. Mineral. Ob-va* **140** (1) 117 (2011)
43. V I Vasil'ev, N V Pervukhina, S V Borisov, S A Magarill, D Yu Naumov, N V Kuratieva *Geol. Ore Depos.* **52** (7) 656 (2010) [*Zap. Ros. Mineral. Ob-va* **138** (2) 75 (2009)]
44. L N Kaplunnik, E A Pobedimskaya, N V Belov *Dokl. Akad. Nauk. SSSR* **251** 96 (1980) [a]
45. L N Kaplunnik, E A Pobedimskaya, N V Belov *Dokl. Akad. Nauk. SSSR* **225** 561 (1975) [a]
46. V Divjaković, W Nowacki *Z. Kristallogr.* **142** 262 (1975)
47. T T Chen, J T Szymanski *Can. Mineral.* **19** 571 (1981)
48. T T Chen, J T Szymanski *Can. Mineral.* **20** 575 (1982)
49. V I Vasil'ev, N V Pervukhina, S V Borisov, S A Magarill *Geol. Ore Depos.* **52** (7) 662 (2010) [*Zap. Ros. Mineral. Ob-va* **138** (2) 83 (2009)]
50. S Graeser, H Schwander, R Wulf, A Edenharter *Schweiz. Mineral. Petrogr. Mitt.* **75** 337 (1995)
51. L Bindi *Acta Crystallogr., Sect. C* **64** i95 (2008)
52. L N Kaplunnik, E A Pobedimskaya, N V Belov *Dokl. Akad. Nauk. SSSR* **253** 105 (1980) [a]
53. L Karanovic, L Cvetkovic, D Poleti, T Balić-Zunić, E Makovicky *Neues Jahrbuch Mineral. Monatsh.* (11) 503 (2003)
54. N V Pervukhina, S V Borisov, S A Magarill, V I Vasiliev, N V Kuratieva, S G Kozlova *J. Struct. Chem.* **51** 898 (2010) [*Zh. Strukt. Khim.* **51** 934 (2010)]
55. V P Glyakin, S V Borisov, M N Tseitlin *Zh. Neorg. Khim.* **33** 303 (1988) [b]
56. I Nakai, D E Appleman *Am. Mineral.* **68** 235 (1983)
57. N V Pervukhina, S V Borisov, S A Magarill, V I Vasiliev, N V Kuratieva *J. Struct. Chem.* **51** 683 (2010) [*Zh. Strukt. Khim.* **51** 712 (2010)]
58. H Yang, R T Downs, G Costin, C M Eichler *Can. Mineral.* **45** 1529 (2007)
59. S V Borisov, S A Magarill, N V Pervukhina *Fundam. Probl. Sovremen. Materialoved.* **8** (1) 31 (2011)
60. S V Borisov, S A Magarill, N V Pervukhina *J. Struct. Chem.* **52** 517 (2011) [*Zh. Strukt. Khim.* **52** 533 (2011)]
61. S V Borisov, S A Magarill, N V Pervukhina *Struct. Chem.* **23** 977 (2012)
62. S V Borisov S A Magarill, N V Pervukhina *Crystallogr. Rep.* **57** 656 (2012) [*Kristallografiya* **57** 735 (2012)]
63. S V Borisov, S A Magarill, N V Pervukhina *J. Struct. Chem.* **53** 734 (2012) [*Zh. Strukt. Khim.* **53** 744 (2012)]
64. S V Borisov, S A Magarill, N V Pervukhina *Fundam. Probl. Sovremen. Materialoved.* **9** (1) 94 (2012)
65. S V Borisov, S A Magarill, N V Pervukhina *Fundam. Probl. Sovremen. Materialoved.* **9** (2) 153 (2012)
66. C V Borisov, S A Magarill, N V Pervukhina *Zap. Ros. Mineral. Ob-va* **142** (4) 118 (2013)
67. S V Borisov, S A Magarill, N V Pervukhina *J. Struct. Chem.* **55** 77 (2014) [*Zh. Strukt. Khim.* **55** 81 (2014)]
68. F Laufek, J Sejkora, K Fejfarova, M Dusek, D Ozdin *Acta Crystallogr. Sect. E* **63** i190 (2007)
69. B Aurivillius *Acta Chem. Scand.* **37** 399 (1983)
70. T Srikrishnan, W Nowacki *Z. Kristallogr.* **141** 174 (1975)
71. S V Borisov S A Magarill, N V Pervukhina, N V Kuratieva, V I Vasiliev *Crystallogr. Rep.* **55** 224 (2010) [*Kristallografiya* **55** 254 (2010)]
72. D Topa, E Makovicky, T Balić-Žunić, W H Paar *Can. Mineral.* **41** 1155 (2003)
73. D Topa, E Makovicky, T Balić-Žunić, P Berlepsch *Eur. J. Mineral.* **12** 825 (2000)
74. T Balić-Žunić, E Makovicky *Can. Mineral.* **45** 437 (2007)
75. G Chapuis, C Gnehm, V Krämer *Acta Crystallogr. Sect. B* **28** 3128 (1972)
76. V Krämer *Acta Crystallogr. Sect. B* **36** 1922 (1980)
77. V Krämer *Acta Crystallogr. Sect. C* **42** 1089 (1986)
78. V Krämer, I Reis *Acta Crystallogr. Sect. C* **42** 249 (1986)
79. V Krämer *Acta Crystallogr. Sect. C* **39** 1328 (1983)
80. L A Olsen, T Balić-Žunić, E Makovicky *Inorg. Chem.* **47** 6756 (2008)
81. D Pinto, T Balić-Žunić, A Garavelli, F Vurro *Am. Mineral.* **96** 1120 (2011)
82. N V Pervukhina, S V Borisov, S A Magarill, N V Kuratieva, N N Mozgova, I V Chaplygin *J. Struct. Chem.* **53** 588 (2012) [*Zh. Strukt. Khim.* **53** 593 (2012)]
83. D Topa, E Makovicky, H Dittrich *Can. Mineral.* **48** 483 (2010)
84. S V Borisov S A Magarill, N V Pervukhina *Crystallogr. Rep.* **56** 935 (2011) [*Kristallografiya* **56** 1001 (2011)]
85. S V Borisov, N V Pervukhina, S A Magarill, N V Kuratieva, I A Bryzgalov, N N Mozgova *Can. Mineral.* **50** 387 (2012)
86. S V Borisov, S A Magarill, N V Pervukhina *J. Struct. Chem.* **53** (Suppl.) S55 (2012) [*Zh. Strukt. Khim.* **53** (Prilozhenie) S58 (2012)]
87. P Orlandi, Y Moelo, I Campostrini, A Meerschaut *Eur. J. Miner.* **19** 267 (2007)
88. D Ginderow *Acta Crystallogr. Sect. B* **34** 1804 (1978)
89. D Pinto, T Balić-Zunić, A Garavelli, E Makovicky, F Vurro *Can. Mineral.* **44** 159 (2006)
90. P Orlandi, A Meerschaut, Y Moelo, P Palvadeau, P Leone *Can. Mineral.* **43** 919 (2005)
91. T Srikrishnan, W Nowacki *Z. Kristallogr.* **140** 114 (1974)
92. D Topa, E Makovicky, T Balić-Zunić *Can. Mineral.* **40** 1147 (2002)
93. W G Mumme, J A Watts *Acta Crystallogr. Sect. B* **36** 1300 (1980)
94. R W Birnie, C W Burnham *Am. Mineral.* **61** 963 (1976)

95. R Euler, E Hellner *Z. Kristallogr.* **113** 345 (1960)
96. V Kupčik *Tscherm. Mineral. Petrograph. Mitt.* **32** 259 (1984)
97. E Makovicky, D Topa, T Balić-Zunić *Can. Mineral.* **39** 1377 (2001)
98. A Meerschaut, P Palvadeau, Y Moëlo, P Orlandi *Eur. J. Miner.* **13** 779 (2001)
99. G Lebas, M-T Le Bihan *Bull. Soc. Fr. Mineral. Crystallogr.* **99** 351 (1976)
100. I V Petrova, L N Kaplunnik, N S Bortnikov, E A Pobedimskaya, N V Belov *Dokl. Akad. Nauk. SSSR* **241** 88 (1978) [a]
101. S V Borisov, N V Podberezskaya, N V Pervukhina, S A Magarill *J. Struct. Chem.* **39** 543 (1998) [*Zh. Strukt. Khim.* **39** (4) 669 (1998)]
102. D Topa, E Makovicky, G Ilinca, H Dittrich *Can. Mineral.* **50** 295 (2012)
103. G Ilinca, E Makovicky, D Topa, G Zagler *Can. Mineral.* **50** 353 (2012)
104. G Ferraris, E Makovicky, S Merlino *Crystallography of Modular Materials* (Oxford: Oxford University Press, 2004)
105. N V Belov *Struktura Ionnykh Kristallov i Metallicheskikh Faz* (Structure of Ionic Crystals and Metallic Phases) (Moscow: Academy of Sciences of the USSR, 1947)
106. W L Bragg, G F Claringbull *Crystal Structures of Minerals* (London: Bell, 1965)
107. S V Borisov, S A Magarill, N V Pervukhina *J. Struct. Chem.* **54** 1070 (2013) [*Zh. Strukt. Khim.* **54** 1039 (2013)
108. S V Borisov, S A Magarill, N V Pervukhina *J. Struct. Chem.* **55** 900 (2014) [*Zh. Strukt. Khim.* **55** 904 (2014)]
109. R Berger *J. Less-Common Metals* **147** 141 (1989)
110. R Berger, L Noren *J. Alloys Compd.* **237** 33 (1996)
111. C L Teske, W Bensch, A Perloff, H Ebert *Z. Anorg. Allg. Chem.* **628** 1511 (2002)
112. R Walther, H J Deiseroth *Z. Kristallogr.* **211** 49 (1996)
113. R Walther, H J Deiseroth *Z. Kristallogr.* **211** 50 (1996)
114. W Bensch, E Woerner *Mat. Res. Bull.* **28** 1005 (1993)
115. M Ohmasa, W Nowacki *Z. Kristallogr.* **134** 360 (1971)
116. T Balić-Zunić, E Makovicky, L Karanović, D Poleti, S Graeser *Can. Mineral.* **44** 141 (2006)
117. M Gostojic *Z. Kristallogr.* **151** 249 (1980)
118. J R Wilson, P K S Gupta, P D Robinson, A J Criddle *Am. Mineral.* **78** 1096 (1993)
119. M E Fleet *Z. Kristallogr.* **138** 147 (1973)
120. G Giester, C L Lengauer, E Tillmanns, J Zemann *J. Solid State Chem.* **168** 322 (2002)
121. S V Borisov, S A Magarill, N V Pervukhina *J. Struct. Chem.* **54** 963 (2013) [*Zh. Strukt. Khim.* **54** 926 (2013)]
122. G V Romanenko, N V Pervukhina, S V Borisov, S A Magarill, V I Vasiliev *J. Struct. Chem.* **40** 270 (1999) [*Zh. Strukt. Khim.* **40** 324 (1999)]
123. V I Vasili'ev, N V Pervukhina, G V Romanenko, S A Magarill, S V Borisov *Can. Mineral.* **37** 119 (1999)
124. N V Pervukhina, S A Magarill, S V Borisov, G V Romanenko, N A Pal'chik *Russ. Chem. Rev.* **68** 615 (1999)
125. S V Borisov, S A Magarill, G V Romanenko, N V Pervukhina *J. Struct. Chem.* **41** 272 (2000) [*Zh. Strukt. Khim.* **41** 335 (2000)]
126. S V Borisov, S A Magarill, N V Pervukhina, N A Kryuchkova *J. Struct. Chem.* **43** 293 (2002) [*Zh. Strukt. Khim.* **43** 317 (2002)]
127. S V Borisov, R F Klevtsova, S A Magarill, N V Pervukhina, N V Podberezskaya *J. Struct. Chem.* **43** 615 (2002) [*Zh. Strukt. Khim.* **43** 664 (2002)]
128. S V Borisov, S A Magarill, N V Pervukhina *J. Struct. Chem.* **44** 441 (2003) [*Zh. Strukt. Khim.* **44** 494 (2003)]
129. S V Borisov, S A Magarill, N V Pervukhina, E V Peresypkina *Crystallogr. Rev.* **11** 87 (2005)
130. N V Pervukhina, S V Borisov, S A Magarill, D Yu Naumov, V I Vasil'ev *Am. Mineral.* **23** 1666 (2008)
131. K Mereiter, J Zemann, A W Hewat *Am. Mineral.* **77** 839 (1991)
132. S A Magarill, S V Borisov, N V Pervukhina, N A Pal'chik *Russ. Chem. Rev.* **76** 101 (2007)
133. N V Pervukhina, G V Romanenko, S A Magarill, V I Vasiliev, S V Borisov *J. Struct. Chem.* **40** 155 (1999) [*Zh. Strukt. Khim.* **40** 187 (1999)]
134. M A Cooper, F C Hawthorne *Can. Mineral.* **41** 1173 (2003)
135. S V Borisov, S A Magarill, N V Pervukhina *J. Struct. Chem.* **50** 312 (2009) [*Zh. Strukt. Khim.* **50** 325 (2009)]
136. E Tillmanns, R Krupp, K Abraham *Tscherm. Mineral. Petrograph. Mitt.* **30** 227 (1982)
137. N A Pal'chik, M Yu Antipin, V I Vasil'ev, K A Potekhin, Yu T Struchkov *Dokl. Akad. Nauk. SSSR* **278** 108 (1984) [a]
138. T J Mormann, W Jeitschko *Inorg. Chem.* **39** 4219 (2000)
139. A L Wessels, W Jeitchko *Z. Naturforsch.* **516** 37 (1996)
140. A L Wessels, W Jeitchko *J. Solid State Chem.* **128** 205 (1997)
141. M S Schriewer-Pöttgen, W Jeitschko *Z. Naturforsch.* **506** 1335 (1995)
142. M S Schriewer-Pöttgen, W Jeitschko *Z. Anorg. Allg. Chem.* **620** 1855 (1994)
143. S V Borisov, S A Magarill, N V Pervukhina *J. Struct. Chem.* **55** 470 (2014) [*Zh. Strukt. Khim.* **55** 500 (2014)]
144. N T Evans *Perspect. Struct. Chem.* **4** 1 (1971)
145. N A Bliznyuk, S V Borisov, L A Glinskaya, R F Klevtsova *J. Struct. Chem.* **32** 876 (1991) [*Zh. Strukt. Khim.* **32** 117 (1991)]
146. S V Borisov, R F Klevtsova *J. Struct. Chem.* **38** 608 (1997) [*Zh. Strukt. Khim.* **38** 732 (1997)]
147. Y P Jeannin, J Martin-Frere *Inorg. Chem.* **18** 3010 (1979)
148. M Nyman *Dalton Trans.* **40** 8049 (2011)
149. F Bonhomme, J P Larentzos, T M Alam, E J Maginn, M Nyman *Inorg. Chem.* **44** 1774 (2005)
150. D Atencio, J M V Couinho, A C Doriguetto, Y P Mascarenhas, J Ellena, V C Ferrari *Am. Mineral.* **93** 81 (2008)
151. M A Cooper, Y A Abdu, N A Ball, P Černý, F C Hawthorne *Can. Mineral.* **50** 793 (2012)
152. M N Sokolov, S A Adonin, P A Abramov, D A Mainichev, N F Zakharchuk, V P Fedin *Chem. Commun.* **48** 6666 (2012)
153. C R Sankar, A Becker, A Assoud, H Kleinke *Inorg. Chem.* **52** 1895 (2013)
154. S V Borisov, S A Magarill, N V Pervukhina *Crystallogr. Rep.* **59** 843 (2014) [*Kristallografiya* **59** 929 (2014)]
155. M Eddaoudi, J Kim, N Rosi, D Vodak, J Wachter, M O'Keeffe, O M Yaghi *Science* **5554** 469 (2002)
156. B Kesanli, W B Lin *Coord. Chem. Rev.* **246** 305 (2003)
157. J S Anderson *J. Chem. Soc. Dalton Trans.* 1107 (1973)
158. J S Anderson *Proc. Ind. Acad. Sci.* **93** 861 (1984)

[a] — *Dokl. Phys. Chem. (Engl. Transl.)*
[b] — *Russ. J. Inorg. Chem. (Engl. Transl.)*